International Journal of Speleology	40 (2)	141-162	Tampa, FL (USA)	July 2011

Available online at www.ijs.speleo.it & scholarcommons.usf.edu/ijs/

International Journal of Speleology

Official Journal of Union Internationale de Spéléologie

Secondary halite deposits in the Iranian salt karst: general description and origin

Michal Filippi[1]*, Jiří Bruthans[2,3], Lukáš Palatinus[4], Muhamad Zare[5] and Naser Asadi[6]

Abstract:

Filippi M., Bruthans J., Palatinus L., Zare M. and Asadi N. 2011. Secondary halite deposits in the Iranian salt karst: general description and origin. International Journal of Speleology, 40 (2), 141-162 Tampa, FL (USA). ISSN 0392-6672. DOI 10.5038/1827-806X.40.2.7

This paper summaries 12 years of documentation of secondary halite deposits in the Iranian salt karst. A variety of secondary halite deposits was distinguished and classified into several groups, on the basis of the site and mechanism of their origin. Deposits formed: i) via crystallization in/on streams and pools, ii) from dripping, splashing and aerosol water, iii) from evaporation of seepage and capillary water, and iv) other types of deposits. The following examples of halite forms were distinguished in each of the above mentioned group: i) euhedral crystals, floating rafts (raft cones), thin brine surface crusts and films; ii) straw stalactites, macrocrystalline skeletal and hyaline deposits, aerosol deposits; iii) microcrystalline forms (crusts, stalactites and stalagmites, helictites); iv) macrocrystalline helictites, halite bottom fibers and spiders, crystals in fluvial sediments, euhedral halite crystals in rock salt, combined or transient forms and biologically induced deposits. The occurrence of particular forms depends strongly on the environment, especially on the type of brine occurrence (pool, drip, splashing brine, microscopic capillary brine, etc.), flow rate and its variation, atmospheric humidity, evaporation rate and, in some cases, on the air flow direction. Combined or transitional secondary deposits can be observed if the conditions changed during the deposition. Euhedral halite crystals originate solely below the brine surface of supersaturated streams and lakes. Macrocrystalline skeletal deposits occur at places with rich irregular dripping and splashing (i.e., waterfalls, places with strong dripping from the cave ceilings, etc.). Microcrystalline (fine grained) deposits are generated by evaporation of capillary brine at places where brine is not present in a macroscopically visible form. Straw stalactites form at places where dripping is concentrated in small spots and is frequent sufficient to assure that the tip of the stalactite will not be overgrown by halite precipitates. If the tip is blocked by halite precipitates, the brine remaining in the straw will seep through the walls and helictites start to grow in some places. Macrocrystalline skeletal deposits and straw stalactites usually grow after a major rain event when dripping is strong, while microcrystalline speleothems are formed continuously during much longer periods and ultimately (usually) overgrow the other types of speleothems during dry periods. The rate of secondary halite deposition is much faster compared to the carbonate karst. Some forms increase more than 0.5 m during the first year after a strong rain event; however, the age of speleothems is difficult to estimate, as they are often combinations of segments of various ages and growth periods alternate with long intervals of inactivity.

Described forms may be considered in many cases as the analogues of forms found in the carbonate karst. As they are created in a short time period the conditions of their origin are often still visible or can be reconstructed. The described halite forms can thus be used for verification of the origin of various carbonate forms. Some of the described forms bear clear evidence of the paleo-water surface level (transition of the skeletal form to halite crystals and vice versa). Other kinds of deposits are potential indicators of the microclimate under which they developed (humidity close to the deliquescence relative humidity).

Keywords: karst, cave, halite, secondary deposit, speleothem

Received 21 January 2011; Revised 12 April 2011; Accepted 20 April 2011

[1] Institute of Geology, Academy of Science of the Czech Republic, Rozvojova 269, 165 00 Prague 6, Czech Republic.

[2] Faculty of Sciences, Charles University in Prague, Albertov 6, 128 43 Prague 2, Czech Republic (Filippi@gli.cas.cz).

[3] Czech Geological Survey, Klarov 3, 118 21, Prague 1, Czech Republic.

[4] Institute of Physics, Academy of Science of the Czech Republic, Na Slovance 2, 182 21 Prague 8, Czech Republic.

[5] Department of Earth Sciences, Shiraz University, Shiraz, Iran

[6] Geology group, Sistan and Baluchestan University, Zahedan, Iran.

INTRODUCTION

Various secondary halite cave deposits have already been described in the literature. For an overview, see the work of Hill & Forti (1997). Secondary halite deposits are usually found in an evaporite rock salt environment (e.g., Rogers 1988; Frumkin, 1992a, b, 1994; Fryer 2005, Giurgiu, 2005; De Waele et al., 2009). However, similar secondary halite deposits also occur in non-evaporite environments (lava tubes, chalk or limestone rocks, etc.) if located in the vicinity of evaporate bearings (e.g., Rimbach, 1963; Lowry, 1967; Forti et al., 1995a; De Waele & Forti, 2010).

The southern and south-western part of the Zagros Mts. represents an area with the largest number of piercing salt diapirs in the world. Dozens of diapirs present a variability of well-developed karst phenomena, including countless salt caves with brine springs and streams and rich secondary halite deposits. Characterization of the karst phenomena and notes on the speleogenesis were presented by Bosák et al. (2002) and the evolution of the surface morphology in relation to the karstification on some coastal salt diapirs was described by Bruthans et al. (2008 – 2010).

Although salt diapirs in this part of Iran represent the largest salt karst areas in the world, the secondary halite deposits have still not been collectively described and characterized. Therefore, this contribution lists all the types of the secondary halite deposits found in the Iranian karst areas and characterizes them according to their morphology and origin. The majority of the described forms are recent; however some may represent evidence of previously predominant conditions. The greatest attention is paid to new or unusual halite secondary forms, which are not known or are only rarely discussed in the literature from other salt karst areas. We also attempt to compare the previously published data with our observations in the Iranian caves to shed new light on general understanding of the formation and transformation of secondary halite deposits. The presented findings are based on extensive field experience from approx. 150 field days spend at diapirs over the last 12 years. Geochemical and mineralogical data are used to support the field observations.

GEOGRAPHICAL AND GEOLOGICAL SETTING OF THE SALT KARST AREAS

The Zagros Mts. are composed of elongated anticlinal limestone oval-shaped ridges, which generally trend NW-SE with principal folding which started only in Middle Pliocene. They contain dozens of piercing salt diapirs with diameter between approx. 1 to 18 km and with circular to elliptical shape. Rock salt composing the diapirs belongs to the Hormoz Complex, which was deposited during Upper Precambrian to Middle Cambrian times (Bosák et al., 1998). The rock salt is folded into tight to isoclinal folds, with alternating white to grayish and reddish salt with varicoloured carbonate, siliciclastic, Fe oxides and volcano-sedimentary rocks and rarely anhydrite. The surface of the visited salt diapirs is usually covered by a broad variety of weathering surficial deposits with thicknesses from several centimeters to several tens of meters (Bruthans et al., 2009). These surficial deposits form a caprock, which prevents many salt diapirs from fast erosion (Bruthans et al., 2008). At the same time, surficial deposits of greater thicknesses, together with large blocks of insoluble rocks, enable collecting of substantial amounts of rain water and subsequent karstification of the underlying rock salt (Bruthans et al., 2000).

In general the salt karst forms are comparable with the common type of karst in carbonate rocks with a wide variety of forms (Bosák et al., 1999, 2001). The caves are passable from ponor to resurgence in many cases, but they mostly terminate by descending below the limit of accessibility due to sediment fill or by breakdown. Old cave levels are rarely preserved due to complete filling by secondary halite deposits and fluvial sediments. Cave passages that have been recently accessible in the Hormoz and Namakdan diapirs are apparently younger than 6000 years, as is indicated by the age of marine terraces and the clear relationship between the cave levels and the surface of the marine terraces (Bruthans et al., 2010).

The climate in the visited areas is arid or semi-arid (Table 1). The 30-year average (1961–1990) precipitation in the coast area is 171 mm (Bandar Abbas station, WMO 2006), but recently average annual precipitation has been less, often just below 100 mm/year (Bruthans et al., 2008, Table 1). Further inland the annual precipitation increases from 100 mm at 300 m a.s.l. to 250 mm at 1500 m a.s.l. (Firuzabad region, 2008-2009 hydrologic years). There are about 15 to 30 rainy days annually (depending on the altitude) concentrated mainly in

Table 1. Measured ion contents in secondary halite deposits and calculated maximum content of gypsum and K-Mg minerals.

sample	S [mg.g^{-1}]	Ca [mg.g^{-1}]	K [mg.g^{-1}]	Mg [mg.g^{-1}]	Content of gypsum (wt.%)	Content of K-Mg mineral (wt.%)
sk1	1.7	3.78	0.77	0.07	0.6	<0.1
sk2	0.38	0.38	0.67	0.03	0.1	0
str	1.8	0.32	3.05	1.36	<0.1	<1.1
tcr	3.59	2.26	2.96	1.18	<0.7	1.0-1.9
sp1	1.99	2.45	0.53	0.08	0.7	<0.1
sp2	2.08	1.89	0.65	0.20	0.6	0.3
gcr1	3.2	3.55	0.33	0.03	1.1	0
gcr2	0.6	0.74	0.45	0.01	0.2	0
gcr3	3.71	3.69	0.63	0.09	1.1	0.1
gcr4	2.82	1.54	1.38	0.41	0.5	0.6
gcr5	3.87	4.52	1.62	0.22	1.4	<0.4

Explanations: sk – skeletal (macrocrystalline) deposits, str – straw stalactite, tcr – thin crust, sp – spray/aerosol deposits, grc – grained (microcrystalline) crust deposits

November-April. The annual average temperature is 27°C in the Persian Gulf Region and 20°C in the mountainous diapirs.

METHODOLOGY

Documentation and sampling in the field

Fifteen salt diapirs and more than 60 salt caves (and adjacent karst areas) have been studied during the past 12 years (for the locations of the most important diapirs: Hormoz, Jahani, Mesijune, Namak, Namakdan, see Fig. 1 and Table 1 in Bruthans et al. (2009). A typical trip to the salt karst area was three weeks long and took place in the winter to spring seasons (in January to May) and under various weather conditions with predominating dry weather but also in periods during and after low and high intensity rainfall (a rain event causing flash-flood with ca 10 years recurrence interval occurred in April 2009). Therefore, we had a good opportunity to observe changes at a single place over time under different conditions. We performed more detailed measurements in selected caves, such as of the temperature and humidity (using a GMH 3350 Greisunger electronic, Germany) and air flow velocity (using Air Velocity Meter TA410). We observed a selected site in the Jahani diapir for three days after the rains to estimate the rate of speleothem growth in the "wet" period of the year.

Samples of various types of secondary halite deposits were collected in the caves and diapirs, dried and stored in plastic bottles and bags. The samples were then studied under a binocular microscope and by other methods.

Instrumental study

Microscopic observations of solid samples were carried out on the OLYMPUS SZX16 binocular microscope with the OLYMPUS SP 350 photocamera. The microphotographs were processed within the QuickPHOTO Micro 2.3 software and Deep Focus 3.0 module.

The surface micro-morphology of various types of halite secondary deposits was studied using the CAMECA SX100 scanning electron microscope. The samples were fixed on a carbon adhesive and plated with gold. Secondary electron imaging (SEI) was performed under the following operating conditions: voltage 20 kV, emission current 90 μA and frame time 60 sec.

X-ray diffraction analyses (XRD) were used for verification of the mineralogical composition of the secondary deposits. The PHILIPS X´Pert PW 3710 diffractometer was employed under the following conditions: CoKα radiation, graphite secondary monochromator, 35 to 40 kV, 30 mA, step scanning at 0.02°/1.1s in the range of 5-80° 2θ; the PDF-2 powder diffraction database was used for peak identification.

A polished section was prepared from a representative sample of a microcrystalline speleothem to evaluate the possible presence of other minerals except the halite. A scanning electron microscope (SEM) VEGA 3XM TESCAN with the BRUKER SDD detector were used. The sample was analyzed under in low vacuum mode without coating.

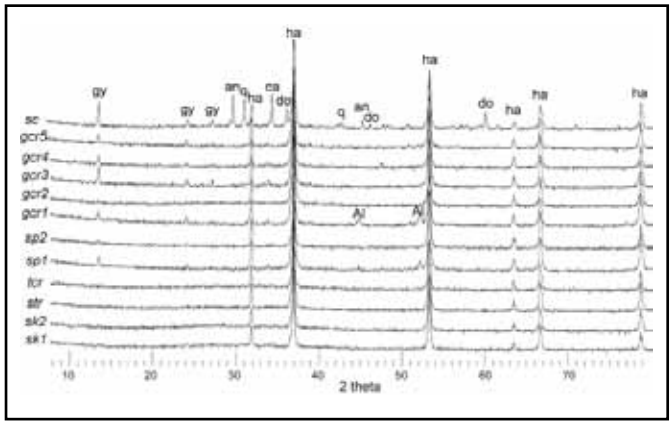

Fig. 1. Set of powder diffraction patterns of various types of secondary halite deposits. Abbreviations: Sk – macrocrystalline (skeletal) stalactite, str –straw stalactite, tcr – thin crust, sp – spray (foam) deposits, gcr – microcrystalline (grained) crust/stalactite, sc – halite crystals from fine sediments (sandy crystals); an – anhydrite, ca – calcite, do – dolomite, gy – gypsum, ha – halite, q – quartz, Al – contamination by Aluminium from the holder.

The chemical compositions of the sampled waters were determined by FAAS (Flame Atomic Absorption Spectrometry - Varian 280 FS) and HPLC (High Performance Liquid Chromatography - Dionex ICS-2000) in the Laboratory of the Geological Institutes (Faculty of Sciences, Charles University in Prague). The speciation and the degree of saturation of the brine waters with respect to the mineral phases were calculated using the PHREEQC geochemical code, version 2.14 (Parkhurst & Appello, 1999). Evaporation of the sampled vadose waters was modeled and the equilibrium with respect to the evaporate minerals was calculated by using PHREEQC with the Pitzer database. Evaporation was simulated in steps. In each step, 10% and later 50% of the remaining water was evaporated. Simulations were performed until 1% of the water remained (99% of the initial water was evaporated). The sequence of the modeled mineral precipitation during the evaporation was noted.

The powdered samples remaining after the XRD analyzes were dissolved in deionized water and analyzed to evaluate the chemical composition of the secondary halite deposits. Determination of Al, Ca, Fe, K, Mg, Mn, P, S, and Si as indicators of possible minor evaporate minerals in the samples was performed by inductively coupled plasma optical emission spectrometry (ICP-OES, IRIS Intrepid II instrument, model XSP DUO).

RESULTS AND DISCUSSION

Air humidity and halite hygroscopicity

Halite is hygroscopic and deliquescent. Thus, it has a strong affinity for water and will absorb atmospheric moisture to form a saturated NaCl solution if the relative humidity (RH) exceeds a threshold called the deliquescence relative humidity (DRH). The DRH for halite is 75% (at 20-30°C; Greenspan 1977). In the Persian Gulf region, the RH of the atmosphere exceeds the 75% threshold in 91% of the daily cycles

(Qeshm Island airport station, years 2002 – 2005), while this threshold is exceeded far less frequently in the mountainous areas on the mainland.

Air with RH > 75% enters the salt caves during 91% of the nights in the Persian Gulf. Atmospheric moisture wets and dissolves halite and slightly dilutes the percolating brine. At the daytime, the RH is < 75% and the brine partly dries out and precipitates halite.

In total, the precipitation of halite clearly dominates its dissolution. Due to the cyclic nature of the process, only small amount of the brine can be formed (max. few milliliters at a given spot) based on our observations of the amounts of humidity condensed on the boulders outside the cave. Only very small salt precipitate features can be formed by this process. A predominant volume of secondary halite is deposited from percolating brine or cave streams.

The temperatures in the visited caves vary between approx. 15 and 30°C in the December to May period. The humidity on the surface and in the caves varied from 25 to 98% and from 52 to 82% respectively (Bruthans et al., 2002 and the new data). The absence of humidity > 82 % in the caves is clearly a result of the depletion of excess moisture in the caves into the halite.

In most of the caves, outside air circulates quickly, causing rapid changes in the humidity and temperature and enabling fast evaporation. The air flow rate often reaches tens of cm/sec and sometimes up to 4 m/s (Polje Cave, Namakdan). The relative air humidity monitored for 22 hours in this intensively ventilated tunnel-like cave varied between 25 and 67%.

Less frequently, the caves have only one opening or very limited size of some passages and thus nearly no airflow. The best example is the upper part of the 3N Cave. The measured values of the air flow velocity were 2-10 cm/s (under conditions with very strong wind at the surface). The temperature and humidity in this cave (with very low ventilation) were logged for 12 hours and the values were stable at 29.3°C and 76-77%.

Composition of saline water (brine)

The composition of the brine, which is the source for halite speleothems was determined in 28 samples of salt springs and streams and 5 drips in the unsaturated zone at five diapirs (Kamas et al., in preparation). Sodium and chloride are the predominant ions, followed by much lower concentrations of sulfate, calcium, potassium and magnesium and other ions. The TDS (total dissolved solids) value of the brine ranges between 255 and 347 g/L. Based on the chemical composition of the brine, the dissolved halite and gypsum form, on an average, 95.7 wt. % and 1.3 wt. % of the brine TDS respectively, and about 3 wt. % is left for other salts composed of K, Mg, SO_4, and Cl.

The sampled brine is mostly saturated with respect to halite, saturated or slightly undersaturated with respect to gypsum and supersaturated with respect to calcite and dolomite. Simulation of evaporation of the brine using PHREEQC (Pitzer database) predicted precipitation of halite after evaporation of 0-10% of the brine. Anhydrite (rather than gypsum) starts to precipitate after evaporation of 0-20 % of the original brine in all the samples. When 50% of the brine has evaporated, it is predicted that glauberite will precipitate in 75% of the samples. When 90% or more of the original brine has evaporated, it is predicted that one or several of the following minerals will precipitate, depending on the water chemistry: syngenite, kainite, labile salt, glaserite, sylvite, bloedite, carnalite, pentahydrite, leonite, schönite, and burkeite.

X-ray results

Twelve fragments separated from various types of secondary deposits were pulverized and analyzed by XRD. The diffraction patterns (Fig. 1) confirmed halite as the major constituent of the secondary deposits. With one exception, the samples did not contain any other minerals except gypsum. The gypsum peaks were repeatedly identified in the patterns of some microcrystalline deposits (speleothems, crusts) that are formed by complete evaporation of the brine and in aerosol deposits. Both these forms are macroscopically monomineral; however, the evaporation of the brine with calcium and sulfate contents results in the crystallization of gypsum, as was confirmed by the SEM study (see below).

The single exception that contains more mineral phases is the macrocrystalline halite from the fluvial sediment, which revealed the presence of anhydrite, calcite, dolomite, gypsum and quartz. These minerals have a general mineralogical composition matching that of the sediments (Bruthans et al., 2009), and are present in the form of sand inside the halite crystals.

Chemical composition of the secondary deposits

Determination of the selected elements in eleven pulverized samples used for the XRD analyses shows that the halite is not entirely pure (Table 1). The maximum possible contents of gypsum in the studied samples of the secondary halite deposits calculated from the Ca and S contents equaled from 0.1 up to 1.4 wt. %. The average content of gypsum (0.7 wt. %) lies at the lower end of its concentration in the brine (0.6 – 1.7 wt. % in 28 brine samples). The high correlation between Mg and K (R^2=0.93) indicates a common source for the two ions. For a high content of Mg, the K/Mg molar ratio is between 2.2 and 3.4, i.e. close to the value of 3.2 for the mineral leonite [$K_2Mg(SO_4)_2 \cdot 4(H_2O)$] and/or picromerite (schoenite) [$K_2Mg(SO_4)_2 \cdot 6(H_2O)$]. Calculated from the content of Mg and limited by the content of K and the remaining sulfate, the non-halite mineral may reach up to 2 wt. % in five samples; its content is below 0.1 wt. % in the other 6 samples (Table 1). Our data clearly indicate that possible non-halite admixtures do not exceed a few percent of the volume of the secondary halite deposits. However, the SEM research performed on the selected microcrystalline sample did not reveal any other mineral except the gypsum present as micro-grains in the halite matter or acicular crystals in cavities (Fig. 2). It follows that other effects, such as the role of the fluid inclusions in the rock salt

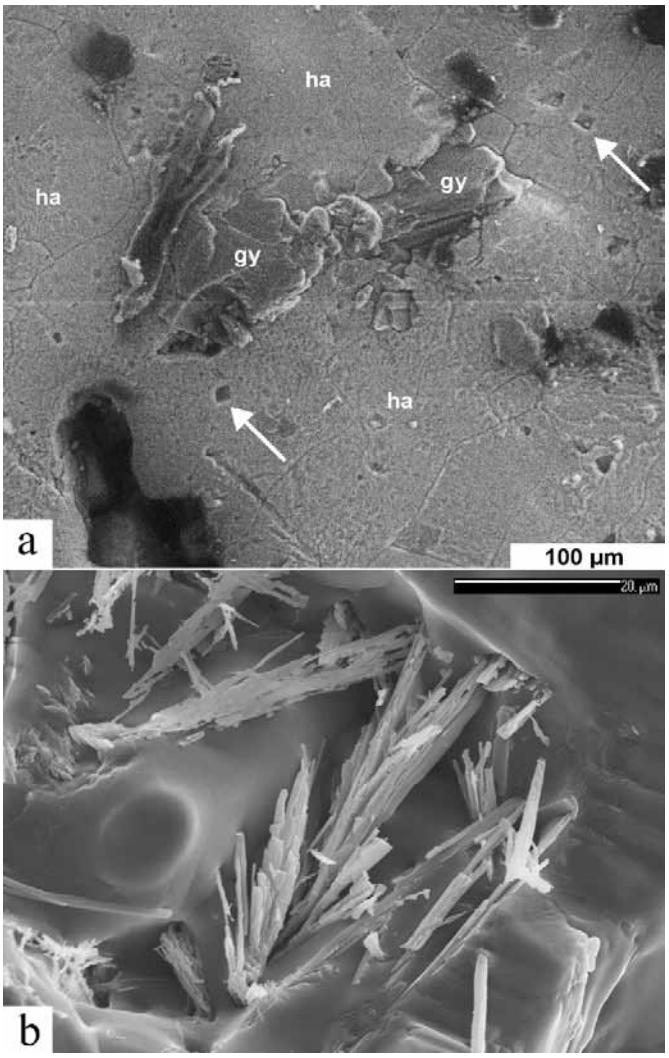

Fig. 2. Gypsum admixtures in microcrystalline halite matrix (gy – gypsum, ha – halite): a) mixed secondary and back-scattered electron photograph showing gypsum grains in halite, the arrows point to the interesting cubic cavities, perhaps originally fluid inclusions; b) secondary electron photograph showing gypsum needles in a cavity.

and probably also in the secondary deposits (see Fig. 2) must be taken into account when explaining the chemical composition of the secondary deposits. These observations point to the need for more detailed research.

Micro-morphology and structure of the secondary deposits

SEM study of the selected samples supports the field observation suggesting two basic types of halite matter: i) more or less compact (crystalline) (Fig. 3a, b, c, d, e) and ii) fine grained (microcrystalline) (Fig. 3f, g, h). Euhedral crystals of different origin (subaqueous, from straws or macrocrystalline deposits) display perfectly smooth compact surfaces and also cores. Still compact, but slightly uneven surface and texture are typical for straw stalactites, thin types of brine surface crusts and aerosol deposits, where accrual layers are also visible. Completely different structure and morphology were documented for all the kinds of microcrystalline deposits. More or less rounded grains up to partly euhedral crystals compose the aggregates of the microcrystalline deposits. Small well-developed cubic crystals may originate in cavities inside the grainy mass at places where the brine was retained for some time. Ageing under slow continual capillary brine inflow may result in recrystallization of grainy halite matter leading to compaction of the structure.

SECONDARY HALITE DEPOSITS

Halite deposits formed via crystallization in/on streams and pools

Subaqueous euhedral crystals

Halite crystallization from supersaturated saline waters in Iranian salt karst areas is caused by evaporation and possibly partly also by declining temperatures (during the night or caused by cool spring water in the winter) (c.f., Cigna 1986; Frumkin & Forti, 1997). Single euhedral crystals already

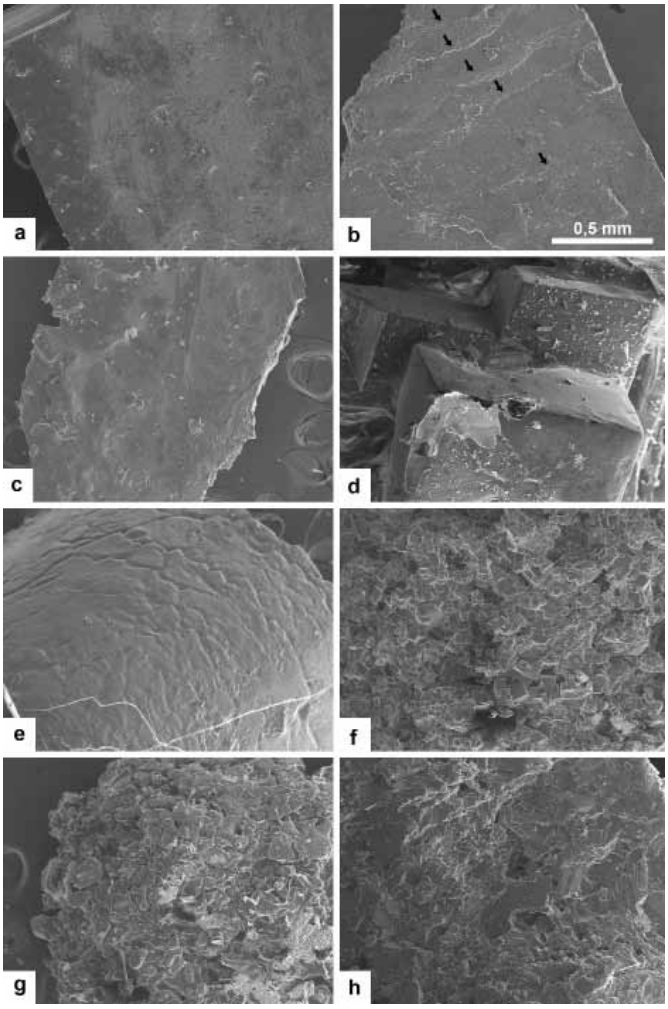

Fig. 3. Secondary electron micro-photographs showing micro-morphology of the surface and/or inner structure of the most common secondary halite deposits: a) perfectly smooth surface of the euhedral crystal from brine pool; b) smooth surface of the microcrystalline brine surface crusts with slightly visible accrual layers (designated by black arrows); c) relatively smooth surface of a straw stalactite; d) cubic halite crystal from the inner side of the straw stalactite; e) rounded surface of aerosol sinter with visible accrual layers; f) inner structure of microcrystalline (grained) crust; g) surface structure of microcrystalline (grained) crust with two acicular crystals of gypsum (near the bottom part of the figure); h) inner structure of the partly recrystallized microcrystalline (grained) stalactite. Scale bar 0.5 mm in part b holds for all the images.

overgrow the stream bottoms inside as well as outside the caves several weeks after the rains. Later, halite crystals agglomerate into extensive crystal crusts and clusters covering the entire stream beds. If the subaqueous crystal accumulations reach the surface of the brine pool, they may form various deposits that are produced by different mechanisms. As a result, association of complex formations including halite films and crusts, shelfstone ledges, rimstones or dams may be observed (e.g., Fig. 4g).

Fig. 4. Subaqueous euhedral crystals originating in the present runoff pools: a) segment of the bottom crystal crust with clear halite crystals up to 3 cm along the edge, 3N Cave, Namakdan; b) segment of the bottom crystal crust with halite crystals containing sand (crystals up to 2 cm along the edge), Fatima Cave, Hormoz; c) up to 2 cm large, separated halite crystals contaminated by ferric ochre on the bottom sediment, Stalactite Forest Cave, Hormoz; d) two generations of halite crystals on the bottom sediment (crystals up to 3 cm along the edge), Stalactite Forest Cave, Hormoz; e) up to 8 cm large parallel halite crystal overgrowing a fragment of rock salt, Stalactite Forest Cave, Hormoz; e) up to 8 cm large parallel halite crystal overgrowing a fragment of rock salt, Stalactite Forest Cave, Hormoz; f) up to 2 cm large halite crystals consisting of an octahedron and cube, Stalactite Forest Cave, Hormoz; g) approx. 15 cm large tower-like cluster of clear halite crystals that was formed on a stone at the bottom of a brine pool in the 3N Cave, Namakdan; h) approx. 1 cm long gypsum needles overgrowing a halite cluster, flooded cenote on the Namakdan.

Larger crystals were generally found in the caves since the evaporation is slower compared to the outer segments of the pool and thus the brine is slightly supersaturated with halite (c.f., Chapter 10 in Palmer, 2007). The crystals (up to approx. 1-3 cm in size, rarely up to approx. 10 cm) are well-developed and regular if the brine surface is undisturbed (Fig. 4a, b, c, d). Irregular, hypo-parallel, fan-organized or partly skeletal development of the crystals is frequent where the water flows rapidly (e.g., Fig. 4e). The prevailing crystal habitus is hexahedral {100}. Sometimes a hexahedron is combined with an octahedron {111}, but hexahedrons prevail and both forms are represented equally only rarely (e.g., Fig. 4f).

Generally, the halite crystals contain few little admixtures of other minerals. However, in 2000 an unusual association of halite with common acicular, up to 3 cm long crystals of gypsum was documented on the Namakdan diapir (Fig. 4h). This association was formed in a slowly dried lake ("cenote") formed in a surficial "gypcrete" environment.

Floating rafts

The occurrence of a floating thin sinter crust, known in the literature as floating rafts, has been observed in carbonate karst on lakes with high HCO_3^- content and rapid decrease in the CO_2 concentration (Palmer, 2007). In the salt karst, floating rafts were described in oversaturated brines from the Mt. Sedom salt diapir (Frumkin & Forti, 1997) or from the Dead Sea (Talbot et al., 1996), and they are also known from other environments, such as the acid saline lakes in Western Australia (Benison et al., 2007). The origin of the salt rafts is different from that of the carbonate rafts, as the salt rafts crystallize due to the supersaturation of the brine via evaporation. Therefore, in the Iranian salt karst, rafts are a common secondary form on the brine surface in cave portals and downstream from them and much less frequent in the deeper parts of caves where the evaporation intensity is lower (Fig.5a).

In the initial stage, very thin flakes of flat (film) halite matter precipitate on the brine surface (Fig. 5b). Floating rafts composed of tightly connected, mostly flattened cubic crystals of translucent halite develop later (Fig. 5c). The sizes of the rafts vary from several mm^2 up to approx. 30 cm^2, i.e. a size of up to approx. 8 x 8 cm. Individual crystals have dimensions of up to approx. 1-2 mm along the edge but are usually smaller. The only observed crystal form is a flat hexahedron. Crystals usually grow in one layer and are parallel with the brine surface and only rarely is a second (often incomplete) layer developed, with unevenly oriented crystals.

In places, where gentle water flow occurs, rafts migrate towards natural halite dams, where they are caught and aggregate into a larger formations (Fig. 5a). If the rafts are too heavy or water flow or wind causes surging, the rafts sink and settle on the pool bottoms. When the pools dry out, all the rafts settle down and are usually overgrown by a microcrystalline halite precipitate (see below) (Fig. 5d).

In the carbonate karst, the calcite film on the water surface can be broken by regular focused dripping and rafts that sink to the bottom may form conical deposits

Fig. 5. Floating rafts: a) closed brine pool in front of the cave – a typical environment for precipitation of floating rafts, 3N Cave, Namakdan; b) floating rafts on the surface of the brine, c) large halite rafts in detail, d) halite rafts deposited on the bottom of a former pool at Namak, e) approx. 20 cm high raft cone in a brine pool, small unnamed cave, Namak.

– cave or preferably raft cones (Hill & Forti, 1997). This form is extremely scarce in the Iranian salt karst and, to our knowledge, no one has so far reported such a form from halite from other sites. Only three raft cones were found in 2007 in an approx. 70 cm deep salt pool. This pool was situated approx. 1.5 to 2.5 m behind the cave outlet of an unnamed cave on the Namak diapir (Geršl et al., 2008). The cave has a limestone bottom and salt ceiling. The documented raft cones, consisting of loose rafts, reached from 15 to 25 cm in height with slopes of 30 to 40° and are situated below the brine surface directly beneath the microcrystalline halite stalactites, whose dripping water probably sank the rafts to form the cones (Fig. 5e).

Crusts and films on the brine surface

Microcrystalline to massive white crusts up to approx. 0.5-1 cm thick form inclined shelfstones on the brine surface, growing from other types of halite formations like aerosol or capillary microcrystalline deposits. They are usually a constituent of more complex secondary formations that gradually develop around/on the brine pools outside the caves (Fig. 6a). The brine surface crusts are composed of superimposed parallel fans (Fig. 6b) and are often slightly inclined downwards due to the decline in the brine surface over time. The surface is either smooth or gently rippled perpendicular to the growth direction and composed of concentric accrual layers made by radially oriented halite crystals or their aggregates. The presence of aerosol results in smoothing of the surface, leading to a glazy appearance (see below section Aerosol deposits and Fig. 3b, e). In contrast, the bottom part of the crust sequence is always concentrically rippled. Those parts in direct contact with brine are composed of flat skeletal crystals if the water is flowing and undulating. Euhedral halite crystals form if the water level is stable.

Transparent films (up to approx. 1 mm thick) formed by very flat (sheet-like, folia) halite crystals are another, relatively rare, form related to the brine surface (Fig. 6c). They border shelfstone deposits. If the water level in the stream is more or less steady (under a constant supply) the crystals grow horizontally. However, if water supply decreases significantly or if the halite films develop in a closed, quickly evaporating pool, decline of the brine surface causes inclined accretion (Fig. 6d, e).

Halite deposits forming from dripping, splashing and aerosol water

Straw stalactites

Straw stalactites grow directly from rock salt or from older secondary halite precipitates on cave ceilings (Fig. 7a, b, c, d). Very often straws are formed

Fig. 6. Crusts and films on the brine surface: a) small rimstone pools/puddles enclosed among the microcrystalline dams – a typical environment for precipitation of thin films and crusts on the brine surface, Jahani; b) white compact crusts growing on the surface of the flowing brine; c) translucent thin halite films on the surface of the undisturbed brine, Jahani; d), e) inclined flat (sheet-like) halite crystals/films above the surface of the evaporated brine, Namakdan.

Fig. 7. Straw stalactites: a) young straw stalactites in the active cave passage, White Foam Cave, Jahani; b) straw column connecting relicts of the destroyed microcrystalline column; many destroyed straws are deposited on the block on the left-hand side, Unwanted Cave, Mesijune; c) the largest documented straw stalactite (length 2.6 m), White Foam Cave, Jahani; d) tip of a partly dissolved (by a flood) older microcrystalline stalactite – a typical environment for the occurrence of young seasonal straw stalactites (length 15 cm), Polje Cave, Namakdan; e) outer part of the straw tube (length 2 cm); f) inner part of the straw tube (length 2 cm).

on the tips of microcrystalline stalactites or on relicts of destroyed (broken, partly dissolved) speleothems. This is caused by reopening of the central channels inside the grained stalactites after the rains. Straw stalactites display more or less uniform diameter (0.5 – 1 cm, rarely more) and a smooth surface composed of compact glazy halite. They commonly have a length of 0.1-1 m, but can reach up to approx. 3 m.

The internal feeding tube of the straw is hollow; however, the inner side is gradually covered by small parallel or skeletal halite crystals precipitating from the flowing brine (Fig. 7e, f). Halite accretion on the perimeter of the tube may be similar as in case of calcite straws (c.f., Stepanov, 1997, Maltsev 1998). First, flat cubic or partly skeletal micro-crystals form at the margins as a result of physical factors during disconnection of the drop (i.e., alternation of evaporation from thin film after disconnection of the drop with accretion from the brine during static hanging of the drop). Later, these are replaced/ completed by the main halite monocrystalline "compact" matter.

In ideal cases, the halite straws are straight and regular, like in carbonate caves. More often, they are irregular, slightly curved and combined with microcrystalline (grained) growths or rarely with filamentary helictites.

Straw stalactites occur in places with rather stable and focused water supply. During their growth, the internal tube is free and the water may descend down to the tip and drip. Later, when the inner part of the straw is filled by halite precipitates and/or if the feed from the rock massif decreases, the brine is retained inside the tube. The brine then starts to seep out through the walls and precipitation of microcrystalline matter will predominate around the primary straw. This situation leads to conversion of the straw stalactite into a microcrystalline speleothem with a typical concentric texture (see the *Origin and succession* section). Preferential growth of the tips against the direction of the wind is observed where groups of straws grow in a windy passage.

Macrocrystalline skeletal deposits

Halite macrocrystalline stalactites have been documented by Fryer (2005) and especially by De Waele et al. (2009), who suggested their origin and mechanism of growth. However, macrocrystalline forms named as "shrub" or "shrubby" speleothems have been known for a longer time from the Polish salt mines (e.g., Dlugosz, 1975). Compared to the rare occurrences studied by De Waele et al. (2009), we had a good opportunity to study this interesting form thoroughly, since it is a very common and active secondary deposit occurring in various environments in the Iranian karst.

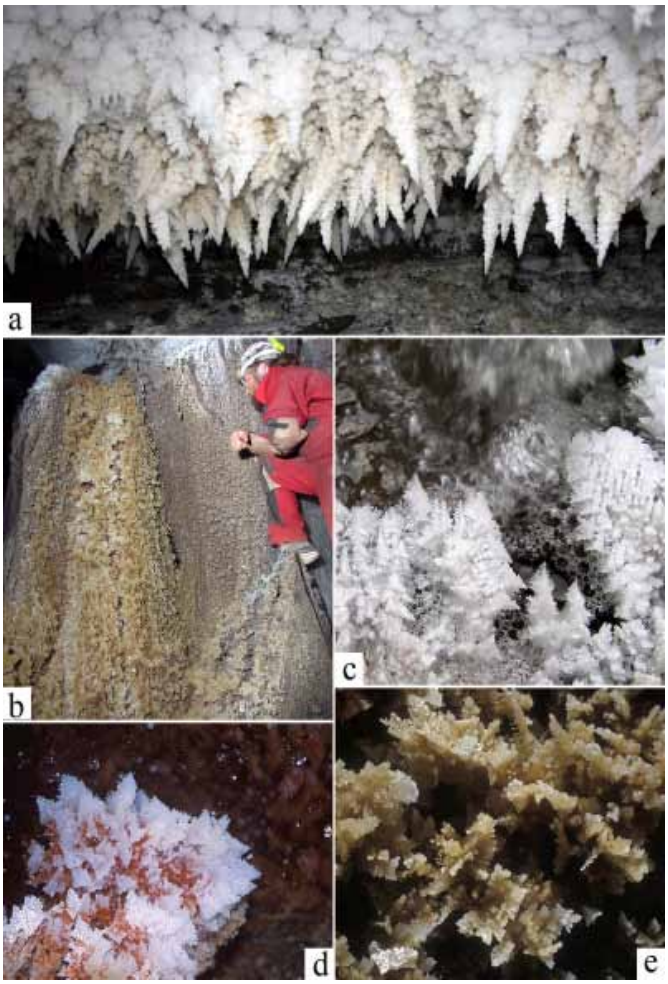

Fig. 8. Typical environments for the occurrence of macrocrystalline (skeletal) deposits: a) cave ceiling with strong brine supply (stalactites are up to 25 cm long), Polje Cave, Namakdan; b) cave wall with a small waterfall, Fatima Cave, Hormoz; c) streambed (dripstone) of a surface stream with wild water and macrocrystalline formations (image cut 50 x 50 cm), Jahani; d) bottom macrocrystalline formation (20 cm in length) close to a small waterfall, Laila Cave, Hormoz; e) a detailed view on the macrocrystalline forms from the situation presented in Fig. 8b.

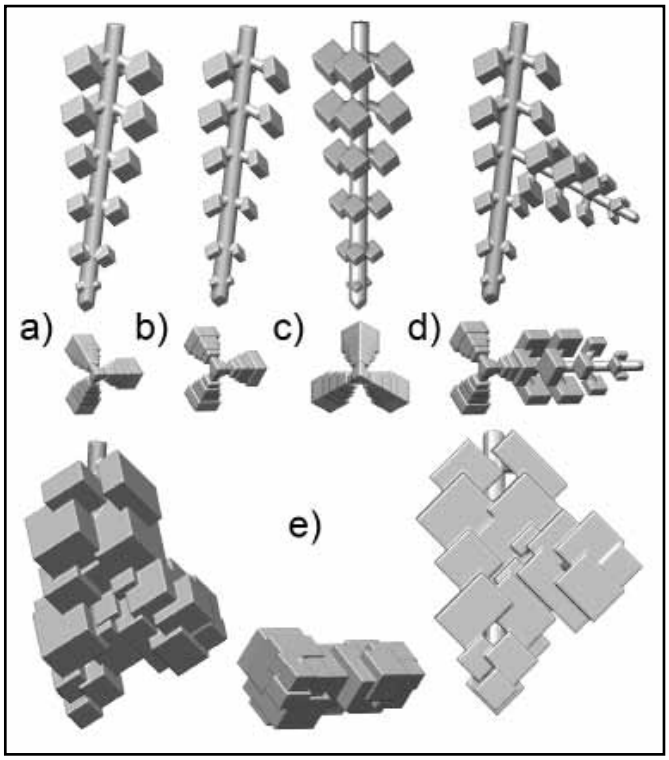

Fig. 9. Models documenting the structure and the growth of macrocrystalline deposits in a lateral view and in a view from below (the skeletal development of the crystals is not included; however, the models were prepared based on the real samples presented in Fig. 10: a) idealized (regular) macrocrystalline stalactite; b) the same stalactite if the cubes are flattened (see also the natural sample in Fig. 10b); c) again the same idealized stalactite in orientation as is presented for the natural sample in Fig. 10a; d) macrocrystalline stalactite with a strongly developed lateral twig (see also the natural samples in Figs. 10g and 10h); e) two lateral views and a view from below on the model of how the cubes are accrued (see also the natural samples in Figs. 10i and 10j).

Macrocrystalline skeletal (sometimes dendritic) forms in the Iranian salt karst are connected to irregularly splashing brine. Rich but more or less random water supply, accompanied by gravity- and capillary-induced water movement, are the main prerequisites for the growth of these halite forms. The evaporation rates at surfaces of the skeletal forms are affected by the presence/absence, direction and velocity of the air flow (including variations in the air density due to temperature and humidity changes).

Splashing of the brine is typical for stream sides and bottoms below/on the waterfalls or for the cave ceilings, ledges and walls with intense water inflow (Fig. 8). Macrocrystalline deposits form stalactites, stalagmites (from several centimeters up to a few decimeters in length) and bottom/wall crusts. These deposits exhibit no internal feeding tube and the brine is distributed on the surface of the deposit. Euhedral to skeletal, mostly irregular and sometimes partly hopper-shaped crystals are clustered into "twigs" forming the whole skeleton/tree-like formations and crusts.

They are translucent to white; rarely, e.g., at the Hormoz caves, they are yellow to red in color due to the presence of hematite ochre in the parent brine. The size of individual crystals varies from 0.1 cm to approx. 3 cm along the edge. The crystals and the whole formations are usually irregularly developed. However, sometimes unique regular dendritic stalactites may be observed. Their forms are very instructive for explanation of the growth of the skeletal stalactites (see Fig. 9).

The idealized skeletal stalactite consists of a central column and side "twigs" growing from the central column (Fig. 9a and Fig. 10a). The central column and the twigs usually have the form of a cylinder, but they are all part of a single halite crystal (in fact – a cluster of identically oriented tightly accreted small cubes whose corners are covered by glazy halite matter).

Fig. 10. Macrocrystalline (skeletal) deposits: a) more or less regular single stalactite, length 3 cm; b) lower part of the same stalactite with the flattened halite crystals and acicular crystals of gypsum (a view from below is depicted in Fig. a, b – tip); c) and d) irregularly developed single stalactites; e) another view on the stalactite in Fig. d) (a view from below is depicted in Fig. d, e – tip); f) more or less regular single stalactite with skeletal crystals, length 8 cm; g) macrocrystalline stalactite with lateral twig and skeletal crystals, length 3 cm; h) macrocrystalline stalactite (with lateral twig) which is overgrown in the upper part by skeletal crystals which cover the early shape, length 10 cm; i) three irregularly developed macrocrystalline forms showing the progress in their growth – the first two samples document the progress of gradual interconnection of the twigs and the third sample shows the skeletal crystal formation and masking of the starting form; the third example is typical for the wall and bottom environments; j) another view of the second form shown in part i) of this figure; k) and l) active complex macrocrystalline formations in situ (length 6 cm and 4 cm, respectively).

This is evidenced by the occasional occurrence of crystal facets of the column and twigs, but especially by the regular distribution of the side twigs around the central axis. The side columns typically occur in groups of three, mutually forming an angle of 120°, with an angle of ~70° to the central column (see Fig. 9 and Fig. 10). The directions of the central and side columns thus correspond to the four body diagonals of a cube – the directions of the fastest growth of halite crystals. Each twig is terminated with a cube. The largest crystals are on the base of the stalactite and the crystal size decreases continuously down-dip (Fig. 9a, b, c and Fig. 10a, b, f). All the cubes are equally oriented, again documenting that the whole form is actually a single crystal, albeit with a fractal appearance (a "fractal cube").

In reality, all sorts of deviations from the ideal shape can be observed. The perfect trigonal symmetry of the whole formation is often broken by the irregular growth in different directions (Fig. 9d and Fig. 10g – 10l). As the form grows more and more, the central column and the twigs can be completely buried under the growing cubes (Fig. 9e and Fig. 10i).

On the samples studied in situ, the upper parts of the cubes are often incomplete (skeletal or hopper shaped), while the lower parts are relatively well developed (Fig. 10). This is caused by the faster and steadier growth from hanging drops at the bottom parts of the cubes. The cubes are generally better developed at places were the brine supply is intense and distinct air draft occurs. The axes of the macrocrystalline stalactites often deviate significantly (up to ~50°) from the gravity vector. The direction of growth is not governed primarily by gravity, but by the orientation of the body diagonal of the cube nearest to the vertical direction. As the initial crystal is oriented randomly, the direction of the nearest body diagonal can deviate from vertical by up to 54°.

At variance with the models proposed by De Waele et al. (2009; Figs. 6b and 8), we observed that all the forms grow primarily along the body diagonals of the fractal cube, and all the faces of the fractal cube are equally oriented regardless of the direction of the growth with respect to the gravity vector.

Except for the rare case of euhedral halite crystals from cenotes (see above), the skeletal halite deposits are the only secondary form where halite is often accompanied by macroscopically visible gypsum. It was detected visually and confirmed by the XRD analysis. Translucent acicular gypsum crystals up to approx. 1 mm long grow randomly from the halite cubes (Fig. 10b).

Macrocrystalline hyaline deposits

Based on the surface morphology and internal fabric, the macrocrystalline hyaline stalactites may be classified as a sort of macrocrystalline stalactite. However, their slightly different appearance and various environmental conditions required for their origin distinguish them from the "common" macrocrystalline skeletal stalactites. Robust hyaline stalactites (Fig. 11) are a rare form that was documented only in the deep parts of the 3N Cave (e.g., from Megadomes, for a cave map see Bruthans et al., 2006), where specific conditions - very low air ventilation and high humidity

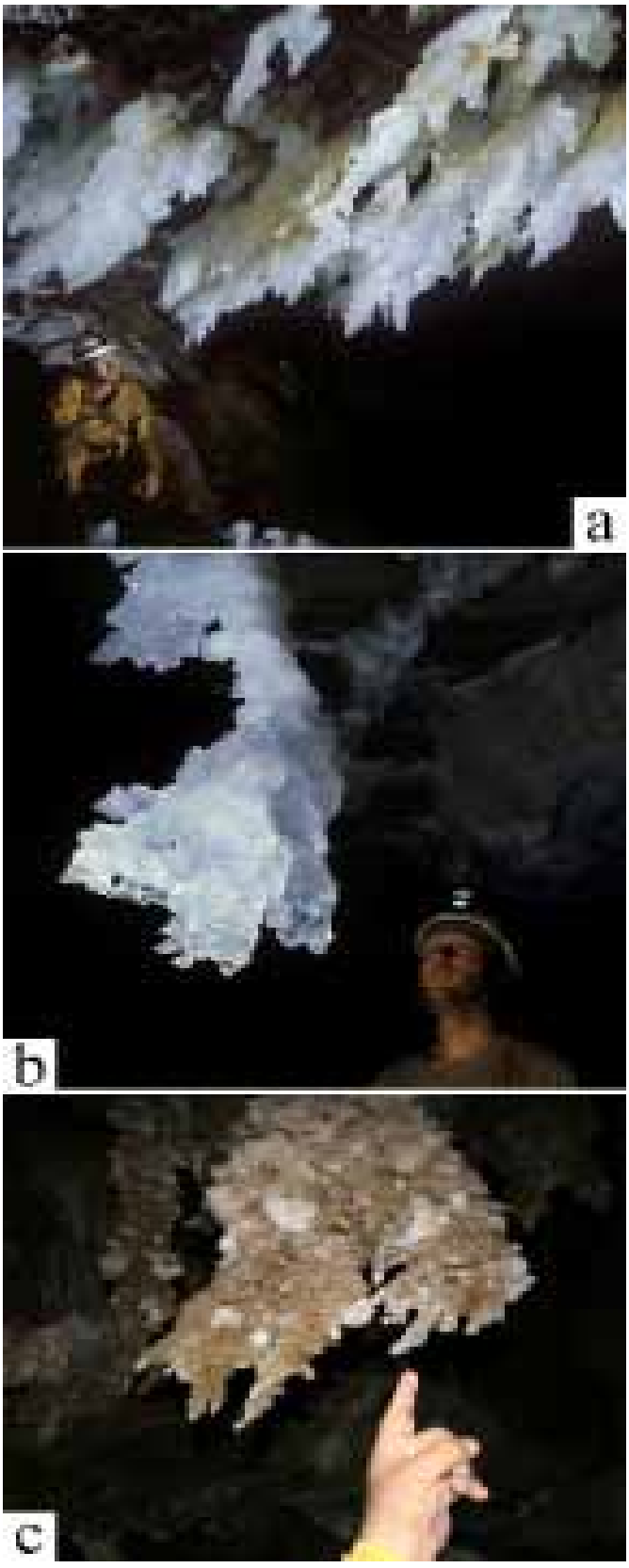

Fig. 11. Macrocrystalline hyaline deposits: a) curtains of the macrocrystalline hyaline stalactites hanging from the ceiling in the cave passage with the air humidity close to DP (3N Cave, Megadomes), Namakdan; b) detail of the pure macrocrystalline hyaline stalactite with the typical cubic symmetry of particular crystals and also the whole formation, 3N Cave (Megadomes), Namakdan; c) detail of the impure macrocrystalline hyaline whose basal part is already overgrown by microcrystalline halite and tip part is still active with imperfect cubic crystals, 3N Cave (Dome by the Octopus), Namakdan.

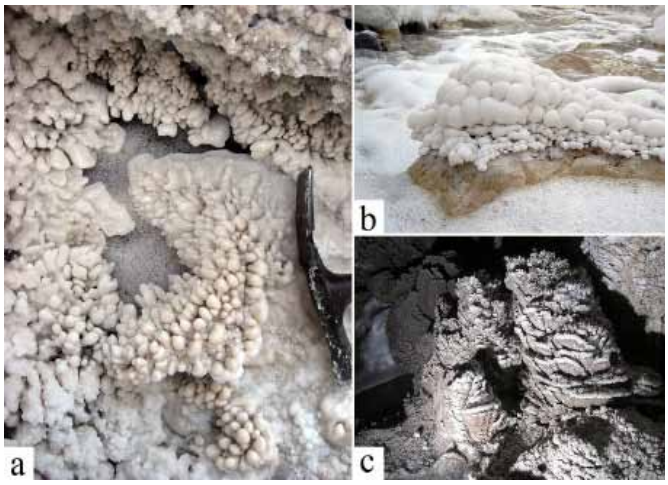

Fig. 12. Aerosol (spray) deposits: a) finger-like (lobbed) deposits forming around the holes in the brine surface crusts covering the rapidly flowing and frothing brine; b) globular deposits on the limestone block above the rapidly flowing and frothing brine; c) complex aerosol sinters around the waterfall in the Waterfall Cave, Jahani.

(close to DRH) - cause extremely slow evaporation. In such an environment, the confluent brine remains as a film on the surface of the secondary formation for long time (active stalactites are wet over most of their surface) and, as the evaporation is very slow, macro-crystals – a transition between the skeletal crystals and euhedral crystals – may form. The supply of brine is not sufficient for the development of perfect euhedral crystals, but suffices for the growth of imperfect, more or less clear, cubic crystals, which are organized similarly to skeletal stalactites. Thick, fine-grained surface deposits overlaying the cave store enough rain water to provide a stable inflow of brine (cf. Fig. 8a in Bruthans et al., 2009).

Aerosol (spray) deposits

Specific lobed or fingerlike formations with a smooth glaze-like surface and white color were observed around small intermittent pools with a specific regime. These pools usually develop in overcrusted streams with small hidden waterfalls or disparities in the streambeds, which both cause surging of the brine with production of foam and very fine spray and aerosol (Fig. 12a, b). The air draft and the deposition of micro-droplets seem to be the crucial factors for the development of these forms (c.f., Maltsev, 1997). The internal parts of the formations are made from concentrically deposited accretion layers, which are oriented towards the source of the aerosol; however, in a short time the layers, although still visible, recrystallize into a macrocrystalline (rough-grained) material – a cluster of single crystals with remnants of the original structure.

The newly described specific halite deposit – halite leaves (blades, fans) formed in columns and wall crusts – found in the surroundings of a waterfall in the Waterfall Cave on Jahani salt diapir (Fig. 12c) have a similar origin but slightly different appearance. The brine falls from a 15 m high underground step and produces clouds of fine aerosol. Unlike in the previously described situation, here the deposit is formed in the cave environment, which is characterized by the absence of sunlight, by the steadiness of the water supply and by relatively stable evaporation rate. As a result, the deposits are more complex and develop for much longer time. Due to the air draft caused by the waterfall, the salty fog settles on the surrounding walls and deposits formations similar to carbonate cave leaves (Jeannel & Racovitza, 1929; c.f. also Fig. 10.32 in Palmer, 2007).

Halite deposits formed from evaporation of seeping and capillary water

Microcrystalline deposits

Secondary deposits consisting of a microcrystalline to grained porous matter are the strongly prevailing type of secondary form in the Iranian salt karst. The microcrystalline deposits reach thicknesses from millimeters up to decimeters. They usually form bowls, ridges and cones and coral- or popcorn-like formation similar to those from the carbonate karst. The surface of the microcrystalline deposits displays various morphologies including floury, pustular or cauliflower-like shapes. The initial microcrystalline deposits that start to form on halite-saturated sites are wet with a glazy compact appearance and with a film of brine on their surface, displaying seemingly light bluish white color. By contrast, the white and clearly grained halite matter precipitates afterwards when the water supply is lower and only capillary transport followed by complete evaporation occurs. The latest halite precipitates forming in the driest periods in the upper parts of deposits are snowy white and loose, usually forming patchy efflorescences.

Generally, microcrystalline deposits precipitate at sites where: i) brine rises from the rock salt to the surface and evaporates (along the bedding planes or fissures in exposed rock salt in caves, along nets of contraction/extension fissures in the surface rock outcrops) and it also borders halite grains (coming from inter-granular spaces); ii) saturated brine seeps due to capillary forces from brine streams and pools into the environment. There are two main environments where this means of transport plays an important role in the production of the microcrystalline deposits. The first are saturated sediments around the brine streams and pools and the second are some cave speleothems that are able to retain water. The following main forms of microcrystalline deposits were documented.

The microcrystalline crusts (called "halite floors" by De Waele et al., 2009) cover all types of unconsolidated and consolidated deposits saturated by brine. They can be found on rock salt, on blocks of exotic rocks in the active riverbeds or on the surface of fluvial sandy sediments. The most common occurrence of microcrystalline crusts is connected with brine springs, streams and pools. They start to grow around springs to form spring domes in later stages. They also occur along the watersides, and seep through the sediments in the vicinity of the streams and pools to form crusts on the surface (Fig. 13a, b, c). Later, with progressive evaporation, the microcrystalline precipitates also protrude as a shelfstone towards the centre of the pools or they form extensive dams (rimstone), reefs and rarely mushrooms similar to those described by Talbot et al.

(1996) (Fig. 13d, e). Sometimes they can form cone- or plate- shaped formations and rims along the cracks on the surface of the dried sediment (Fig. 13f, g). In many places with cyclic flooding (e.g., in front of large cave outlets), microcrystalline crusts compose large multi-generation formations that consist of old corroded deposits and new ones (Fig. 20a, b). The formation of microcrystalline crusts on (close to) the brine surface is a complex process that is closely connected with halite precipitation below the water level combined with capillary transport (vertical growth) if the subaqueous deposits grow above the brine surface.

Fig. 13. Microcrystalline crusts: a) white secondary salt crusts forming spring domes in places where brine rises onto the diapir surface, Namak; b) crusts covering non-evaporite sediments around the brine stream leaving the Mesijune; c) crusts covering limestone background around the brine stream leaving the Namak; d) typical rimestone dams in a brine stream composed by microcrystalline halite, Fatima Cave, Hormoz; e) shelfstone and plates (mushrooms) in a stream leaving the 3N Cave, Namakdan; f) microcrystalline crusts with cone formations on the bottom of the brine stream leaving the 3N Cave, Namakdan; g) crusts with fractures around the brine stream leaving the Mesijune.

Microcrystalline stalactites and stalagmites

Microcrystalline stalactites are very common secondary forms in the Iranian salt karst and also in other salt karsts around the world. They reach up to approx. 3 m in length and are sometimes curved and furcated (Fig. 14). The initial formation of microcrystalline stalactites is also primarily related to the presence of dripping water; however, evaporation of capillary water is the key factor governing their growth. Microcrystalline stalactites are actually the successive form of deposits that started to grow by dripping or splashing water.

Usually, the microcrystalline stalactites form only when the water feed decreases so that capillary transport prevails over gravitational dripping. This is the stage when the "primary" forms finish their development. In fact, microcrystalline stalactites are mostly the second stage in the secondary halite deposition (cf., De Waele et al., 2009). Therefore, remnants of the original forms can be observed in the cross-sections of microcrystalline stalactites – partly filled central feeding tube (e.g., former straw stalactite, Fig. 14g) or irregular (often three) small cavities located between the former "crystal twigs" of the macrocrystalline skeletal stalactites.

Microcrystalline stalactites are usually not exactly vertical but are curved or zigzag shaped (Fig. 14a, b, c, d). Several directions of stalactites may be observed at one place in the cave. This is caused by the shape of the original form and by successive development, i.e. periodic changes in the shape at the tip of the stalactite (see the *Origin and succession* section). Outer factors, such as the air draft direction or spatial distribution of the atmospheric humidity are also significant. The stalactites are often oriented against the direction of the wind draft (in the winter season we measured a draft velocity of up to approx. 4 ms^{-1}). Therefore, faster halite precipitation on the draft-ward sides is probable. Microcrystalline stalagmites are much scarcer secondary forms in caves and their constitution is more complex, reflecting several periods of the development (Fig. 14e, f).

Microcrystalline helictites

Curved filamentary helictites formed by evaporation of capillary brine were found on the surface

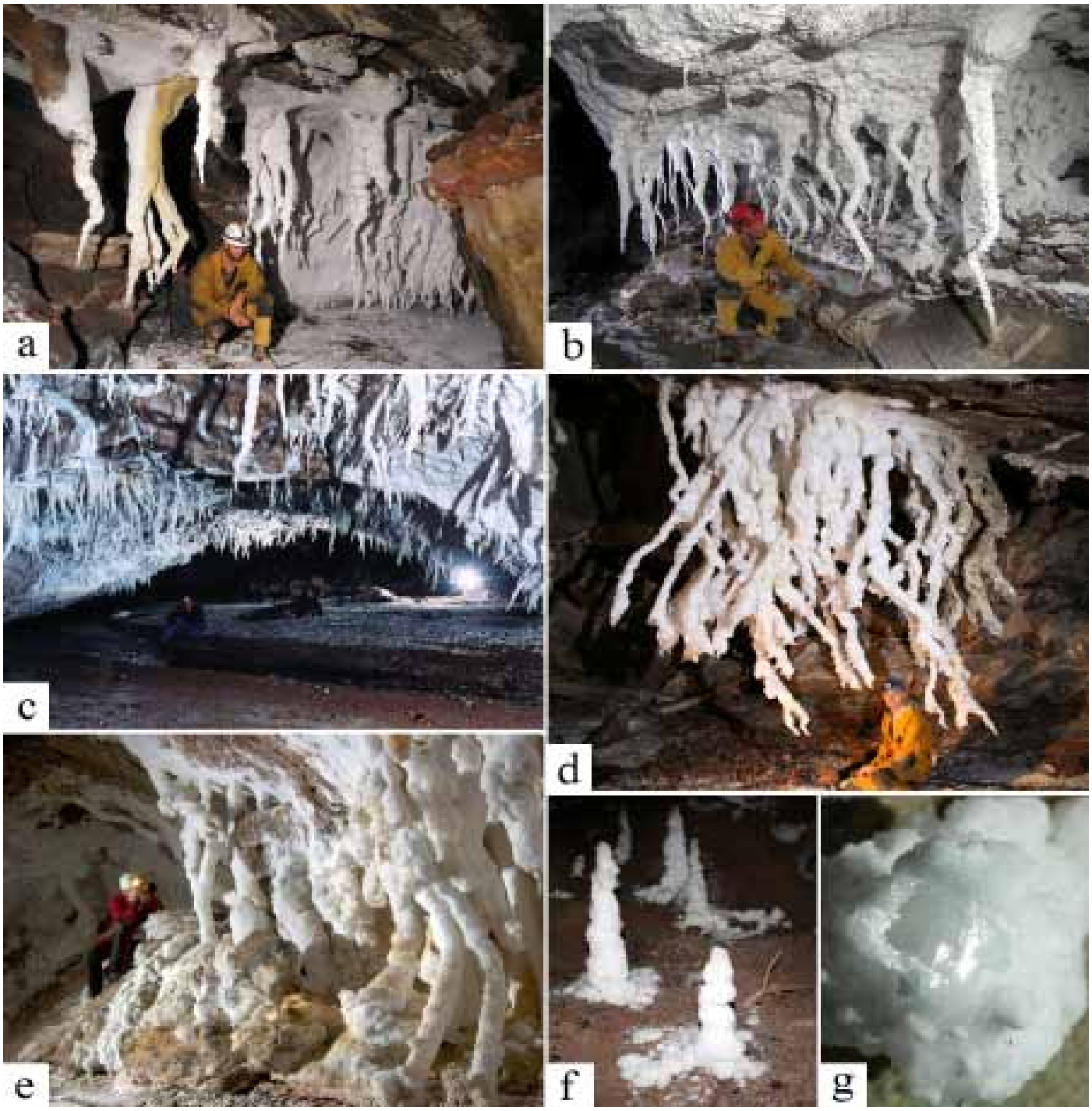

Fig. 14. Microcrystalline stalactites and stalagmites: a) typical microcrystalline stalactites (simple or furcated and some rarely colored by Fe oxides) in a medium-sized passage, Fatima Cave, Hormoz; b) zig-zag microcrystalline speleothems in a passage with changing air flow direction, Canyon Cave, Namak; c) typical microcrystalline stalactites dispersed on the roof in a large-sized passage, Namaktunel Cave, Namakdan; d) rare rich cluster of long furcated stalactites; e) massive sinter columns by the side of the large passage, both examples from the 3N Cave, Namakdan; f) stalagmites on the fluvial sediments in the Upper Entrance Cave, Namakdan; g) cross-section through the tip of a young microcrystalline (grained) stalactite with visible internal tube of the former straw stalactite.

of some young microcrystalline stalactites that were formed from recently closed straws (Fig. 15a). Similar, strongly warped helictites were also found on the surface of wet microcrystalline bottom/wall crusts or sediments (Fig. 15b). Generally, this form is relatively scarce in the studied areas. In accordance with Frumkin & Forti in Hill & Forti (1997) or De Waele & Forti (2010), we found that the growth of the halite helictites is connected with the air draft. Helictites were documented in cave portals or in other places in caves with substantial air flow. At the surface, helictites may be observed on the tops of saturated halite deposits, e.g., on microcrystalline crusts around the stream beds, in notches and small narrow valleys with air currents, etc. (Fig. 15c). On straw stalactites, helictites may be oriented in one or two preferred directions based on the prevailing distinct air draft; elsewhere (where the air draft is not obvious), they are completely chaotic. Their length usually does not exceed 1 cm, but can occasionally reach up to approx. 10 cm. The width is constant from approx. 0.5 up to approx. 1 mm.

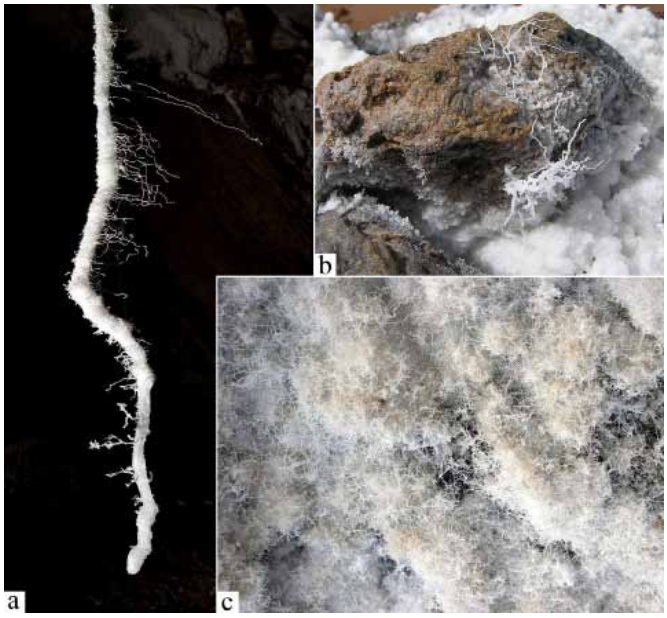

Fig. 15. Microcrystalline helictites: a) up to 8 cm long helictites growing from the closed straw stalactite, Polje Cave, Namakdan; b) up to 4 cm long helictites growing on non-evaporite stone close to the brine puddle, entrance to the Namaktunel Cave, Namakdan; c) rich and very thin cover of helictites on the floor of a rock salt canyon, Namak.

Other forms

Peculiar forms of secondary halite deposits can sometimes be observed at various places in the Iranian salt karst. It may be quite difficult to recognize their origin if their early stage is not found or if the process of their formation is no longer active. Below we list some examples of these anomalous deposits.

Halite bottom fibers and spiders

Cave fibers and spiders usually formed by gypsum are interesting cave formations known especially from limestone-sulfate karts areas (Hill & Forti, 1997). Fan-organized, root or bundle (looking like spiders or "conversed shrublets") halite fibers found in the Iranian salt karst are related to fine-grained fluvial sediments at old cave levels and in areas occasionally flooded by ponds with slow fine sedimentation from the suspension. These unusual halite formations create fragile 1-3 cm long fibers and blades and their aggregates cover the surfaces of upper sedimentary positions around occasionally active streams (Fig. 16a). The internal structure of each fiber indicates that it is essentially an imperfect halite single crystal stretched in the vertical direction. In some places, the sediment was first covered by thin halite crusts in the form of a very flat (0.5 mm thick) translucent film and later the bundle/spider forms precipitated beneath the crusts.

Up to 10-20 cm high and 30 cm wide fibrous clusters were very rarely found on fine sediments in old passages (currently above the highest flood level) in the 3N Cave (Fig. 16b, c). Similarly to the gypsum "flowers" and "spiders" mentioned from several caves around the world (see Hill & Forti, 1997), the halite formations grow from the outermost layers of the sediment and therefore push the older halite precipitates outward. Later, when the formation

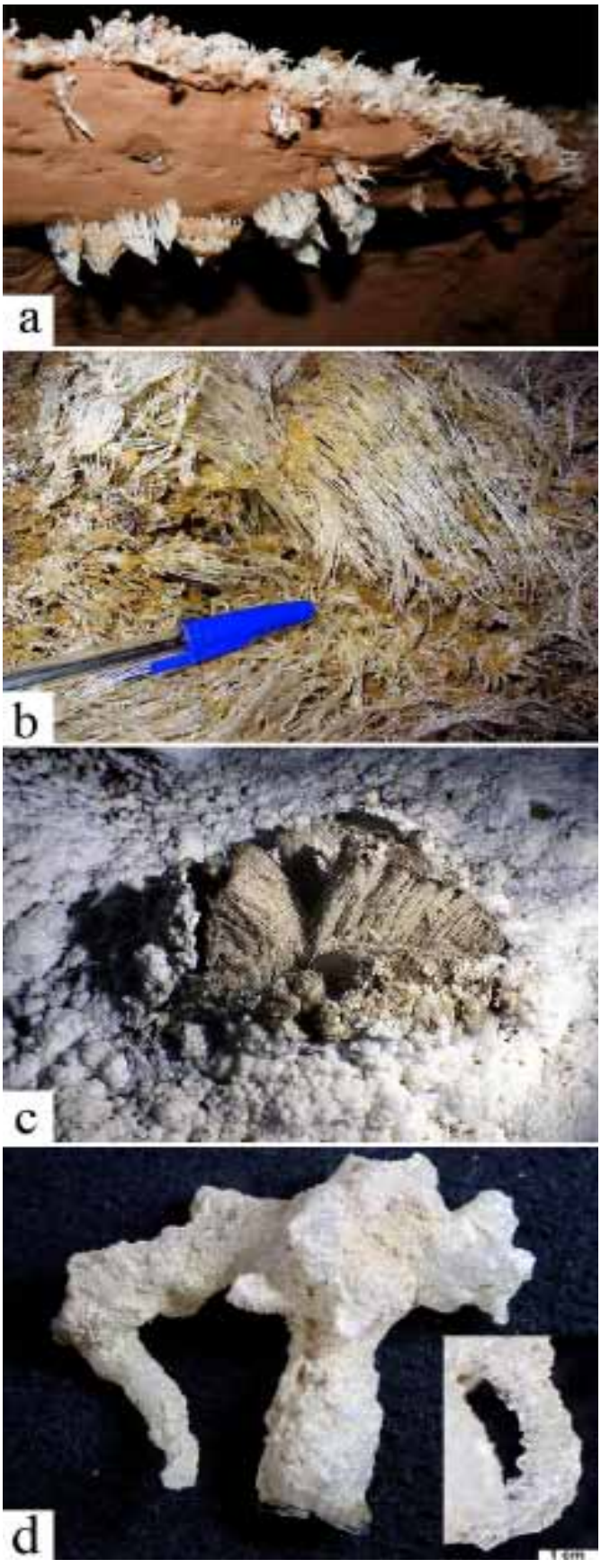

Fig. 16. Other forms – bottom fibres, spiders and macrohelictites: a) up to 2 cm large "spiders" on a wet fine fluvial sediment in the Upper Entrance Cave, Namakdan; b) up to 4 cm long halite fibres from the cave passage with air humidity close to DP (3N Cave, Megadomes), Namakdan; c) up to 10 cm long bottom fibres in the Snow Passage, 3N Cave, Namakdan; d) approx. 5 cm large macrocrystalline helictite from old (inactive) level in the 3N Cave, with detail of the surface.

Fig. 17. Other forms – crystals in the fluvial sediments and in the rock salt: a) relatively clear irregular halite crystals from clay fluvial sediment (approx. 8 cm in the longer axis), 3N Cave, Namakdan; b) cluster of approx. 2 cm large halite crystals from coarse sandy layer enclosing sand inclusions; c) well developed halite crystals (up to 3 cm in the edge) in a rock salt fissure, Tchula's Lair Cave, Jahani; d) typical cluster of the crystals/grains from fully filled fissure in the rock halite; e) approx. 1 cm large halite crystals with unusually shapes {210} and perhaps {111}, pool in the 3N Cave, Namakdan.

becomes too high, it loses its stability and falls down on the sediment to form a loose "snowy" layer.

The small fibers and shrublets in active parts of the Upper Entrance Cave grew within one year (Fig. 16a). On the other hand, the large fibrous copulas in old horizons in the Snow Passage (3N Cave) may have been growing up to several hundreds of years, as these parts were not directly flooded by streams in the last 600 years (radiocarbon dating, Bruthans et al., 2010, sample K2). While the fibers are protected from dissolution by flood water, they may grow due to capillary rise of brine through the fine sediments and they are probably still growing, at least after flood events, which inject water into the underlying sediments.

All these forms are found in an environment with humidity close to the deliquescent point of halite.

Macrocrystalline helictites

This extremely rare form was found and sampled in 1999 in an old part of the 3N Cave close to the occurrences of halite fibers. Two collected samples were found lying on the bottom in fine fluvial sediment in a long-inactive passage (old level + 2 m). Both samples consist of coarse-grained to crystalline aggregates, which compose a vermicular to finger-like formation (Fig. 16d). Due to the lack of experience with this form, we are not able to reliably describe its origin.

Crystals in fluvial sediments

Relatively well-developed, clear to gray halite crystals and crystal clusters (Fig. 17a, b) were occasionally found in fine-grained fluvial sediments in the humid parts of the 3N Cave (e.g, Namakdan highway, Megadomes; humidity close to the deliquescent point of halite). Several centimeters in size, sometimes partly skeletal or cross-shaped cubes grew displacively in partially compacted sandy-clay sediment, perhaps recycling some previous halite deposits (c.f., Naiman et al., 1983). Halite crystals and their clusters locally form irregular bearings with an area of several of m^2. Samples from coarse sandy layers enclose large amounts of sand inclusions and are thus cloudy with rough surfaces. The appearance of halite crystals forming old sediments in the 3N Cave resembles the familiar gypsum desert roses.

Fig. 18. Combined or transient forms: a) approx. 2 cm large white skeletal formation enclosed in an euhedral halite crystal; b) skeletal formation overgrowing the euhedral halite crystal, both examples come from the Stalactite Forest Cave, Hormoz; c) white aerosol sinters enclosed in a transparent halite crystal aggregate, Jahani; d) aerosol sinter (left amorphous part of the formation) covering the skeletal sinter, White Foam Cave, Jahani; e) inactive macrocrystalline (skeletal) sinters partly overgrown by a microcrystalline halite, Canyon Cave, Namak; f) approx. 20 cm long young (1 year) closed straw stalactites at the tips of damaged stalactites are gradually overgrown by a microcrystalline halite matter, Polje Cave, Namakdan; g) globular aggregates composed of microcrystalline halite matter growing on straw stalactites in places where the internal tube was filled by precipitates, Canyon Cave, Namak.

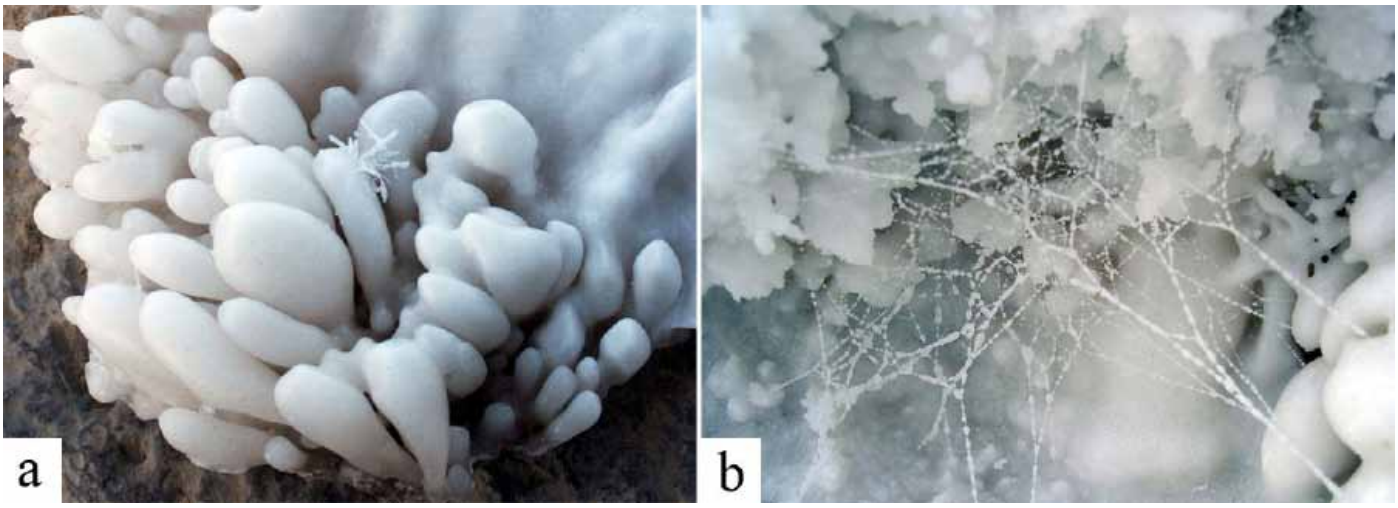

Fig. 19. Biologically induced deposits: a) aerosol sinter with the plant seed covered by halite; b) spider web in the spring crusts, both examples come from the Jahani.

The "sandy halite crystals" occur in layers. They grow from brine slightly oversaturated with respect to halite in the sediment and form more or less irregular cubes or skeletal formations close to the water surface but within reach of capillary rise from upward flow of soil moisture, similarly to the gypsum desert roses (e.g., Watson, 1985). Oscillation of the brine surface and later supply of moisture derived from floods, together with grain–size variation in the sedimentary layers, may be the main factors influencing the crystal shape and amount of sand inclusion. Compared to the halite crystals formed in brine or by dripping, those in sediments most probably grow for a much longer time, perhaps hundreds of years.

Euhedral halite crystals in rock salt

Well-developed halite crystals up to several centimeters (rarely decimeters) in size were found at several diapirs (e.g., Hormoz, Jahani, Mesijune) in cavities of the fissures in rock salt walls in caves (Fig. 17c, d). These fissures are usually completely filled by halite and therefore the crystals did not retain their crystal faces and are clustered into large coarse-grained aggregates with single crystal cleavage of each grain. If the crystals are terminated by crystal faces, only cubes are present, not octahedrons, similar to crystals from oversaturated streams. The crystals often contain brine inclusions in cubic or oval cavities. Frumkin & Forti in Hill & Forti (1997) described crystals from a similar environment from the Liquid Cave in Israel and suggest their origin under phreatic conditions prior to the development of the cave. However, these cavities could also be a result of the deformation of the salt mass and fracturing in the close surroundings of existing large cave halls. Created fissures may be filled by brine seeping through the rock to the cave. As the salt is plastic below the brine surface and even huge mine cavities are quickly closed by rock salt flow (Warren, 2006), it is hard to explain how a cavity could be kept open below a major brine surface (beneath the cave level).

Euhedral halite crystals derived from rock salt grains

Unique halite crystals were found in the 3N Cave in the winter of 2000. Unusually developed euhedral crystals up to approx. 2 cm in size and their rare aggregates were found in a cave pool which was situated below the corroded cave ceiling: grains of rock salt that dropped from the ceiling into the brine were overgrown by new material and formed crystals with tetrahexahedrons {210} and octahedrons {111} (Fig. 17e). To our knowledge, this is the first observation of tetrahexahedra on crystals of natural halite.

Combined or transient forms

Some secondary halite deposits may exhibit combined or transient forms as a result of sudden or slow changes in the external conditions. Overgrowth of the older halite secondary formation by a younger one (created by a different mechanism) is the most common case. An illustrative example could be a skeletal formation that primarily originated on stones above the brine surface and later sank into the brine and was overgrown by perfectly developed, translucent halite crystals (Fig. 18a). The opposite example was also documented. Halite crystals that developed in the brine were overgrown by a skeletal continuation when halite crystals were exposed above the brine surface (Fig. 18b). Similarly, if fingerlike deposits created by the spraying brine are quickly flooded by brine, they are overgrown by clear euhedral crystal matter (Fig. 18c). Covering of the macrocrystalline dendritic form by compact "aerosol-deposited" halite is another example of changing water supply (Fig. 18d).

A straw or macrocrystalline stalactite overgrown to a variable extent by microcrystalline halite is the commonest example of a form created by a succession of two different processes (Fig. 18e, f, g). Another transient form is related to the ceiling macrocrystalline hyaline deposits and was documented in parts of the 3N and Upper Entrance caves with very low air ventilation and humidity close to DRH. Crusts and stalagmites with the appearance of solidified dripping wax originate from brine dripping from the cave

ceiling and splashing over the bottom. The perfectly smooth surface of the formation and absence of visible crystals faces (compared to the macrocrystalline hyaline forms) is probably caused by a combination of skeletal growth with spraying brine. However, lack of occurrences of this rare deposit prevents the more precise characterization.

Biologically induced deposits

Dozens of species of fauna and flora live in the Iranian salt karst. Sometimes living organisms and products of their metabolism or activity are dipped or spilled into the brine and become a substrate for the precipitation process. Relicts of plants, spider webs or small dead animals overgrown by halite are among the most frequent examples. If the biological material is fully overcrusted and combined with the common speleothems, it can confuse the investigators studying its origin (Fig. 19).

ORIGIN AND SUCCESSION OF FORMATION OF SECONDARY HALITE DEPOSITS

Rapid precipitation of secondary halite deposits is clearly connected with the winter/early spring periods after heavy rains when meteoric water traverses surface and underground streams, percolates via surface deposits and rock salt and later drips in a cave environment. In the summer, in contrast, potential evaporation during the day is higher but a sufficient amount of water is not available.

Formation of the secondary halite deposits has spatial dependence and a certain succession. Straw stalactites grow at places where the supersaturated water emerges in one place when dripping from cave ceilings. Macrocrystalline or aerosol deposits develop if the water sprays into the environment. All these forms are closely connected to periods shortly after rains. Euhedral crystals and floating rafts form later when pools develop due to blocking of streams by precipitating halite dams. Well-developed subaqueous crystals grow especially in caves where brine supersaturation with respect to halite is low and constant, which evokes a small number of crystallites and thus gradual enlargement of the crystals. On the other hand, sunshine and stronger ventilation outside the caves causes quick supersaturation, especially in the upper layer of the water pools, and therefore small crystals forming numerous rafts rapidly precipitate.

Microcrystalline forms grow much longer and often continuously as they are supplied by a permanent or slowly depleting source (brine stream, soil moisture). Common overgrowing of straws and macrocrystalline deposits by microcrystalline matter is an effect of a decrease in flow, which is no longer able to supply gravity water and only capillary water remains. In other words, the microcrystalline (grained) forms are the final stage of secondary halite deposition. This corresponds to the suggestions of Maltsev (1998), who

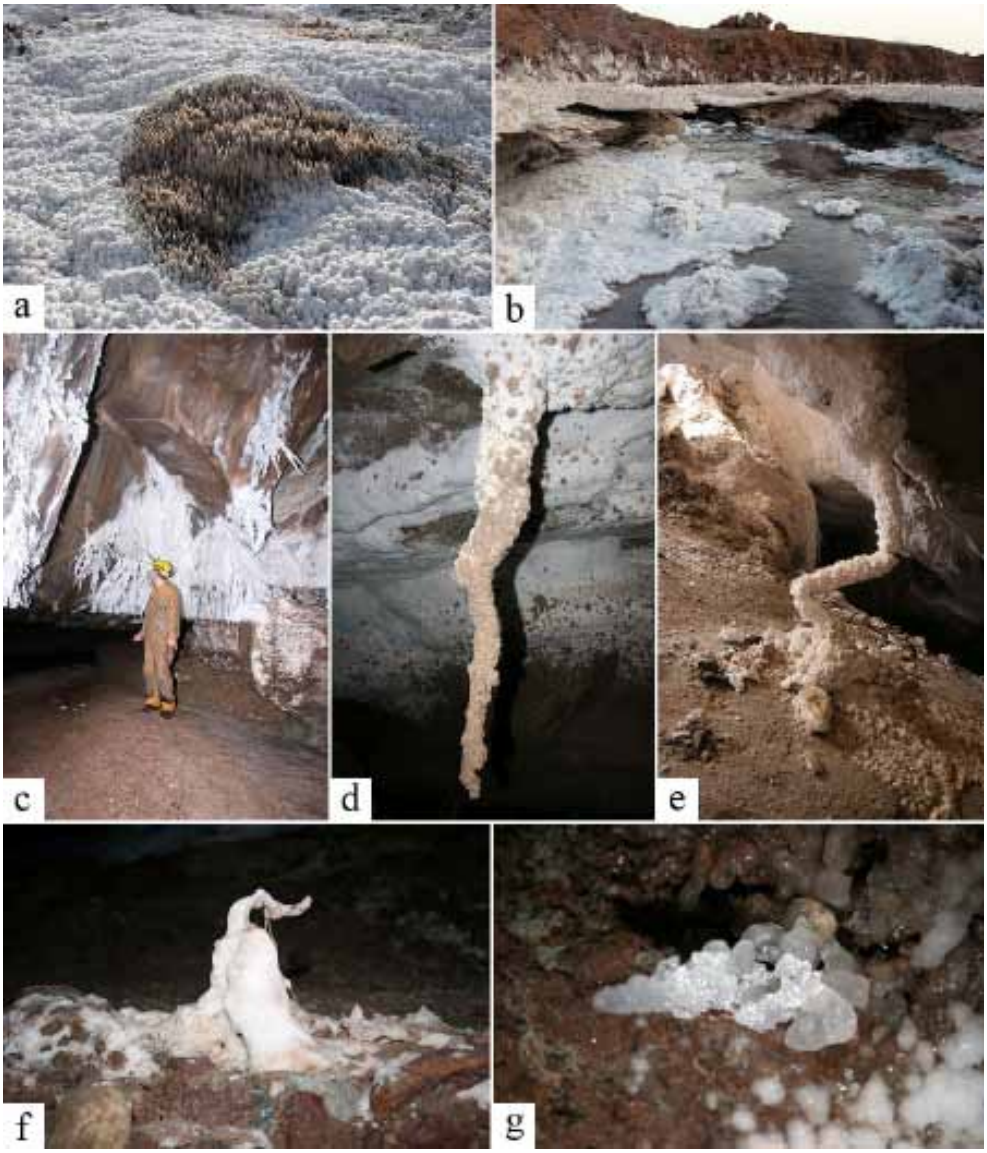

Fig. 20. Destruction of secondary halite deposits: a) older (brown) spring dome crust with Rillenkarren made by rain is slowly overgrown by fresh (white) microcrystalline precipitate, Namak; b) older (brown) stream crust (shelfstone) is slowly overgrown by fresh (white) microcrystalline precipitate, stream leaving the 3N Cave, Namakdan; c) microcrystalline stalactite cut by flood, 3N Cave, Namakdan; d) microcrystalline sinters contaminated by mud from wild stream during the flood, entrance part of the Waterfall Cave, Jahani; e) a sinter column probably cracked due to the rock salt movement, Canyon Cave, northern glacier of the Namak diapir; f) stalagmite mostly dissolved by flooding; g) dripping hole in a macrocrystalline hyaline stalagmite made by unsaturated brine, both examples from the Upper Entrance Cave, Namakdan.

concluded that the importance of evaporation for the speleothem morphology increases with a decrease in the dripping frequency.

Microcrystalline forms, as the most common type of secondary deposits formed by capillary transport, followed by evaporation, occur widely on the surface of the diapirs and in caves where at least minimal air flow occurs (i.e., in caves with a short length or with a number of connections with the surface). In caves with low air flow and air humidity close to DP (= deliquescent point) (closed caves, old cave levels) the deposition is slow and secondary deposits are scarce. Bottom crusts are not developed even several years after the last flood in Megadomes and another part of 3N Cave where the atmospheric humidity is close to DRH.

Rate of growth and age of the secondary halite deposits

Generally, the precipitation processes in the salt karst are much faster compared to the carbonate areas.

However, growth rates depend on the type of halite deposit, on the air draft and the climate (temperature, humidity). Solar radiation, air flow and temperature increase the evaporation and thus accelerate the precipitation; on the contrary, humidity close to DRH has an inhibitive effect.

At the Jahani diapir, selected straws and skeletal stalactites were observed over 3 days, approx. 20 days after a major rain event. The flow rate and length of the stalactites were measured (Table 2). The stalactites were situated at the bottom of a 10 m deep shaft, but still within reach of direct sunshine for part of the day. Table 2 shows that the straws and skeletal stalactites were elongated at a similar rate (2-5 mm/day). The drip rate was higher in the case of the skeletal stalactites, but the highest drip rate was measured for a straw terminated by a several mm long skeletal outgrowth inside the drop of water at the end of the straw. We can very roughly estimate that just a few percentage of the dissolved halite arriving at the stalactites was precipitated, the rest being carried out by dripping brine.

Table 2. Elongation and drip rates measured for straws and skeletal stalactites. The last column gives the ratio of estimated weight increase of stalactite in 3 days/total amount of dissolved NaCl passing the tip of the stalactite.

Type of deposit	Drip rate [mL/day]	Elongation in 3 days [mm]	Elongation rate [mm/day]	Rough estimation of precipitated NaCl out of brine
Straw	4	10.5	3.5	3 %
Straw	13	9	3.	-
Straw	18	6.5	2.2	1 %
Straw	44	-	-	-
Straw	51	12	4	0.2 %
Straw + macrocrystalline	883			
Macrocrystalline + microcrystalline	142	11	3.7	4 %
Macrocrystalline	55	10	3.3	10 %
Macrocrystalline	176	-	-	-
Macrocrystalline	189	14	4.7	3%
Macrocrystalline	195	-	-	-
Macrocrystalline	242	-	-	-
Macrocrystalline	288	-	-	-
Macrocrystalline	591	-	-	-

- not measured

Based on these measurements, we can expect elongation of stalactites in order of centimeters up to first decimeters within weeks to months after the major rain event. This estimation agrees well with our observations from repeated visits to the same places in caves, where we found stalactites elongated in range of 10 to 30 cm (occasionally up to approx. 50 cm) after one year.

Similarly, microcrystalline sinters bordering the streams precipitate very quickly. Their growth starts immediately after the rain and continues for a long time until moisture in the sediments is depleted.

Because of rains, the cyclical growth and the destruction of bottom deposits (microcrystalline crusts, euhedral crystals, folia, rafts, etc.) can be observed at many places. Old forms are damaged or fully removed and new forms develop at the same place or on relicts of the older deposits. Therefore, the majority of secondary formations within reach of flood waters are less than several years old, as they are destroyed by every flood. Stream beds, ceilings in low caves and occasional spring domes are typical examples.

In contrast, gradual accretion (increase and overgrowths) is typical for other places, where much older deposits can be documented. These secondary halite deposits are found out of the reach of flood waters, in upper cave levels, on/in old fluvial sediments in the caves or on high cave ceilings. Owing to the low stability of the cave ceilings and fast halite accrual (thus weight increase), gravitational collapsing of the cave ceiling or part of stalactite is the major factor limiting further growth of the ceiling- and wall- deposits. Stalactites are thus often a combination of very old and younger segments. We suppose that the older segments of stalactites are often several tens or hundreds of years old. For example, stalactites in the Namaktunel Cave on the Namakdan diapir damaged by visitors in 1999 have not recovered over past 12 years).

Possibly very old halite deposits are connected with old fluvial cave sediments. Based on radiocarbon dating of wood pieces in sediments from similar levels in caves, the age of sediments bearing crystals is between 3 and 6 thousand years (Bruthans et al., 2010). In addition, on the surface of several studied salt diapirs (Jahani, Khurgu, Namak, etc.), we found fragments of various more or less solidified fine-grained sediments (mostly mudstones) containing displacive hopper-shaped quartz pseudomorphs after halite, or cubic, often deformed cavities, sometimes filled by hematite or dolomite. Therefore, it is obvious that halite was a common subaerial chemogenic precipitate (c.f., Gornitz & Schreiber, 1987; Benison et al., 2000; Pope & Grotzinger, 2003) pointing to saline depositional environments also in the more distant geological history of the diapirs.

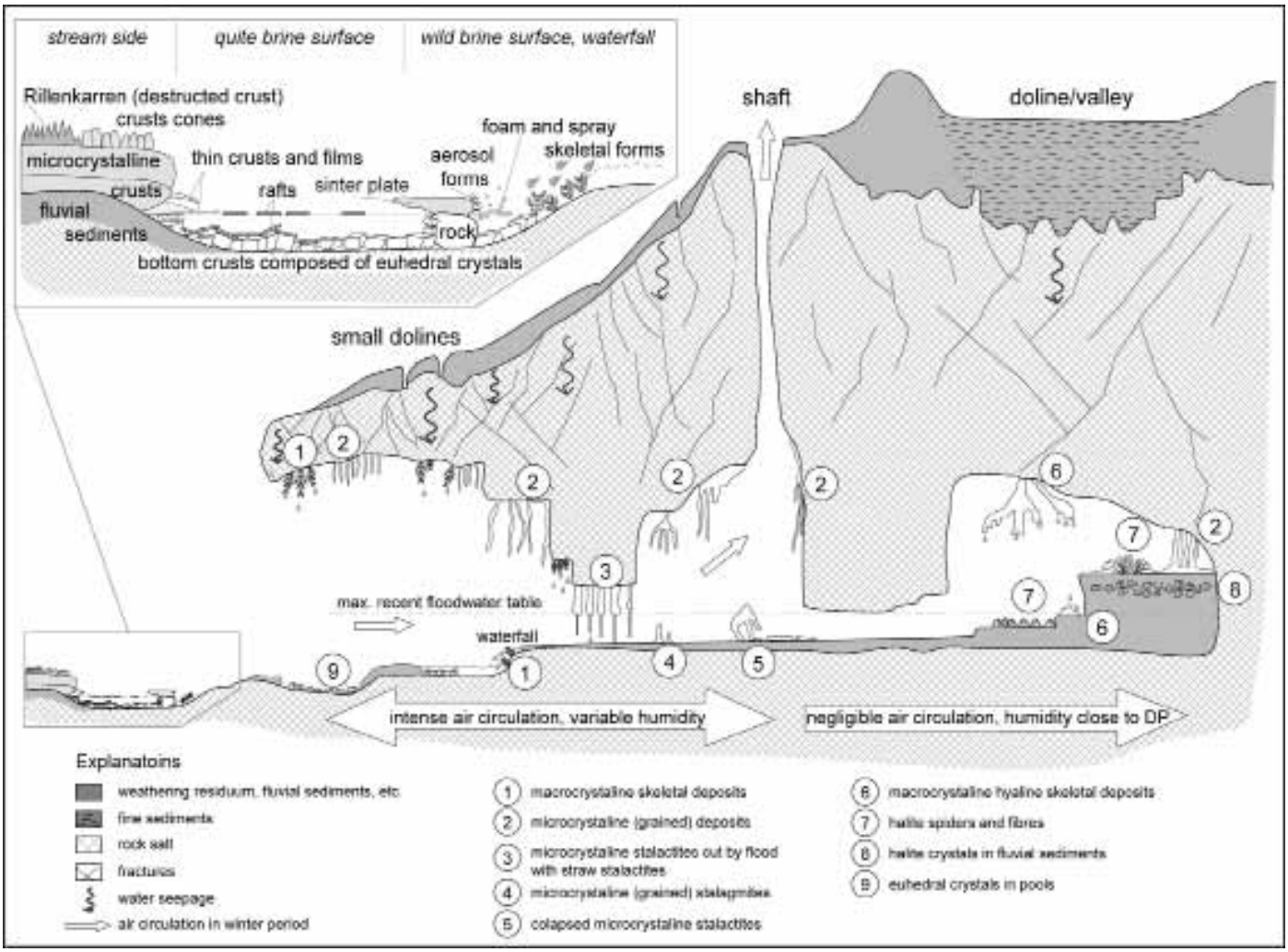

Fig. 21. A simplified model of a salt cave (inspired by the 3N Cave) with various secondary halite deposits and the dependence of their occurrences on the environmental conditions.

Destruction of secondary halite deposits

Most commonly, destruction is a direct effect of heavy rains and floods. Until the dissolution remnants of secondary deposits are fully recovered, they constitute newly developing secondary forms and differ from the original deposit in their shapes. For example, the surface microcrystalline crusts are corroded by rains and modeled into corrosion rillenkarren (Fig. 20a, b). Microcrystalline stalactites growing in the narrow spaces in caves are often "cut" by floodwaters undersaturated with respect to halite (Fig. 20c). Wild splashing muddy floodwater may also contaminate halite deposits above the brine surface by non-evaporite minerals (Fig. 20d). Stalactites and stalagmites immersed in the corrosive water for only a short time are partly dissolved and formed into bizarre "amorphous-like" shapes (Fig. 20f). We also documented inner corrosion of large microcrystalline stalactites due to the supply of unsaturated water into the free spaces in the stalactites.

Collapsing of the extensive and thus heavy secondary precipitates from the cave ceilings is another common type of destruction, perhaps sometimes related to infiltration of rain/surface water into the rock salt massive. The fallen blocks are quickly dissolved by floodwaters so they do not accumulate in the cave.

Cracking and breaking constitute a common destructive mechanism in the case of straws and slim microcrystalline stalactites when these reach a cave floor (Fig. 7a, b). Therefore, similarly as in the carbonate karst, fallen fragments of straws may be found on cave bottoms between the flood events. Situations when stalagmites are only cracked and remain in the same place curved in a sharp angle are rare and often it is not clear if this is an effect of deposit growth or gradual descending of the cave ceiling. In some specific cases, stalagnates are cracked and clearly bent with open fractures, but still not collapsing. Most probably the ceiling moved gradually down, and the space between the ceiling and the bottom of the passage was reduced by 30% or more. The fractures were cemented by the precipitates from the percolating brine. The cracked column in the Canyon Cave at Namak diapir may be a result of differential movement of the salt mass as a whole (Fig. 20e).

A few stalagmites with narrow deep holes caused by water dripping from the cave ceiling were documented in the Upper Entrance Cave in April 2010 several days after strong rains (Fig. 20g). Stalagmites were found in places where the cave ceiling was rich in layers of coarse-grained non-evaporite admixtures, often with stones derived from the magmatic and sedimentary rocks. Neither stalactites nor other secondary halite

precipitates were present on the ceiling. Therefore, we suppose that non-evaporate layers are able to feed water unsaturated with respect to halite for some time, which dissolved secondary deposits on the bottom deposited in former depositional periods.

CONCLUSIONS

More than 30 caves with the surrounding karst areas situated on 15 salt diapirs in the Zagros Mts. (Iran) have been visited (most of them repeatedly) and the secondary halite deposits have been documented. The various types were distinguished and characterized based on their morphology, internal fabric and origin. The spatial distribution of the particular forms of halite deposits strongly depends on the character and intensity of brine inflow (source of halite) and on the physical conditions affecting supersaturation and crystallization – namely on the spatial and temporal pattern of the evaporation rate, which is a function of sun radiation, air flow, air humidity, temperature and other factors (see model on Fig. 21).

Secondary halite deposits were classified, based on the site and mechanism of their origin, into several basic groups. Deposits forming: i) via crystallization in/on streams and pools, ii) from dripping, splashing and aerosol water, iii) from evaporation of seepage and capillary water, and iv) other types of deposits. The following examples of halite forms were distinguished in each of the above-mentioned groups: i) euhedral crystals, floating rafts (raft cones), thin brine surface crusts and films; ii) straw stalactites, macrocrystalline skeletal and hyaline deposits, aerosol deposits; iii) microcrystalline forms (crusts, stalactites and stalagmites, helictites); iv) macrocrystalline helictites, halite bottom fibers and spiders, crystals in fluvial sediments, euhedral halite crystals in rock salt, combined or transient forms and biologically induced deposits.

Successive development of the secondary deposits was documented. Straw stalactites, macrocrystalline and aerosol deposits are tightly connected to periods shortly after rains. The euhedral crystals and floating rafts form later when pools have developed due to blocking of streams by precipitating halite dams. Microcrystalline forms grow much longer and often continuously, as they are supplied by a permanent or slowly depleting source. Common overgrowing of straws and macrocrystalline deposits by microcrystalline matter is an effect of flow decrease that is no longer able to supply gravity water and only capillary water remains. The rate of growth was documented and measured to reach up to several decimeters after the rain event. The age of the individual forms can range from weeks to hundreds of years.

Some of the described forms bear clear evidence of the paleo-water surface level. Dating these forms of halite in old mine/geological deposits can thus be used to distinguish whether a specific place was situated below or above the water level, and to determine the position of the paleo-water surface level. Other kinds of deposits are also possible indicators of the microclimate in which they developed (e.g., humidity close to DRH) and they can therefore assist in the reconstruction of the cave paleo-climate.

This contribution extends knowledge about already known secondary halite deposits, but also provides data about new and as-yet unpublished forms. Our field observations concerning the origin of the secondary halite may hold generally for other salt karst areas and may also explain secondary halite formation in already inactive salt karsts.

In many cases, the described forms seem to be analogues of forms found in the carbonate karst. As they are created in a short time period, the conditions of their origin are often still present or can be reconstructed. The described halite forms thus can be used for verification of the origin of various carbonate forms.

ACKNOWLEDGEMENTS

The authors wish to thank the Vice-Chancellor of Shiraz University, Head of the International Section of Shiraz University in Qeshm and Head of the Qeshm Free Zone Organization for their support during the field works in Qeshm and Hormoz islands. The authors would also like to thank M. Audy, R. Bouda, O. Jäger, J. Kukačka, Š. Mikeš and T. Svoboda for providing valuable photographs from the field. This research was supported by project No. KJB315040801 of the Grant Agency of the Academy of Sciences of the Czech Republic and by Institutional Research Plan No. AV0Z30130516 (Institute of Geology, AS CR) and research project MSM00216220855 (Charles University in Prague) and MZP0002579801 (Czech Geological Survey)**.** The authors would also like to thank the Českomoravský Cement Co. (Heidelberger Cement Group) for financial support in 2003 and 2006 and the partners of the Expedition foundation in 2010. Finally, the authors appreciate the suggestions of the reviewers (one of them P. Forti), which helped to improve the first version of the manuscript, and M. Štulíková is greatly acknowledged for improving our English.

REFERENCES

Benison K.C., Bowen B.B., Oboh-Ikuenobe F.E., Jagniecki E.A., LaClair D.A., Story S.L., Normále M.R. & Hong B.-Y., 2000 - *Sedimentology of acid saline lakes in southern Western Australia: Newly described processes and products of an extréme environment*. Journal of Sedimentary Research, **77**: 366-388.

Benison K.C. & Goldstein R.G., 2007 - *Sedimentology of ancienit saline pans: an example from the Permian Opeche Shale, Williston Basin, North Dakota, U.S.A.* Journal of Sedimentary Research, **70 (1)**: 159-169.

Bosák P., Jaroš J., Spudil J., Sulovský P. & Václavek V., 1998 - *Salt Plugs in the Eastern Zagros, Iran: Results of Regional Geological Reconnaissance*. GeoLines, **7**: 1-174.

Bosák P., Bruthans J., Filippi M., Svoboda T. & Šmíd J., 1999 - *Karst and caves in salt diapirs, SE Zagros Mts., Islamic Republic of Iran*. Acta Carsologica, **28 (2)**: 41-75.

Bosák P., Filippi M., Bruthans J., Svoboda T. & Šmíd J., 2002 - *Karstogenesis and speleogenesis in salt diapirs: Case study from the SE Zagros Mts., Islamic Republic of Iran*. Proceedings of the Middle-Eeast Speleology Symposium (MES), 20-21 April 2001: 62-79.

Bruthans J., Šmíd J., Filippi M. & Zeman O., 2000 - *Thickness of cap rock and other important factors affecting morphogenesis of salt karst*. Acta Carsologica, **29 (2)**: 51-64.

Bruthans J., Filippi M., Šmíd J. & Palatinus L., 2002 - *Tří Naháčů and Ghar-e Daneshyu Caves - The world´s second and fifth longest salt caves*. The International Caver 2002: 27-36.

Bruthans J., Filippi M., Zare M., Asadi N. & Vilhelm Z., 2006 - *3N Cave (6580 m): Longest salt cave in the world*. The NSS news. National Speleological Society, **64 (9)**: 10-18

Bruthans J., Asadi N., Filippi M., Vilhelm Z. & Zare M., 2008 - *Erosion rates of salt diapirs surfaces: An important factor for development of morphology of salt diapirs and environmental consequences (Zagros Mts., SE Iran)*. Environmental Geology, **53 (5)**: 1091-1098.

Bruthans J., Filippi M., Asadi N., Zare M., Šlechta S. & Churáčková Z., 2009 - *Surficial deposits on salt diapirs (Zagros Mts. and Persian Gulf Platform, Iran): Characterization, evolution, erosion and influence on landscape morphology*. Geomorphology, **107**: 195-209.

Bruthans J., Filippi M., Zare M., Churáčková Z., Asadi N., Fuchs M. & Adamovič J., 2010 - *Evolution of salt diapir and karst morphology during the last glacial cycle: effects of sea-level oscillation, diapir and regional uplift, and erosion (Persian Gulf, Iran)*. Geomorphology, **121**: 291-304.

Kamas J., Bruthans J., Jäger O., Asadi N., Zare M., Filippi M., & Mayo A., in preparation -*Hydrogeology of salt diapirs in the Zagros Mts. Iran: Field study, isotopes and chemistry*. Hydrogeology Journal.

Cigna A. A., 1986 - *Some remarks on phase equilibria of evaporites and other karstifiable rocks*. Atti Simp. Internazionale sul carsismo nelle evaporiti, Le Grotte d´Italia, **12**: 201-208.

De Waele J., Forti P., Picotti V., Galli E., Rossi A., Brook G., Zini L., Cucchi F., 2009 - *Cave deposits in Cordillera de la Sal (Atacama, Chile)*. In: Rossi P.L. (Ed.), *Geological Constrains on the Onset and Evolution of an Extreme Environment: the Atacama Area*. GeoActa. Special Publication, **2**: 97-111.

De Waele J. & Forti P., 2010 - *Salt rims and blisters: peculiar and ephemeral formations in the Atacama Desert (Chile)*. Zeitschrift für Geomorphologie, **54**, Suppl. 2: 51-67.

Dlugosz A., 1975 - *Muzeum Zup Krakowish Wieliczka*. Wydawnicza Krakow. 39 p. (in Polish)

Fryer S., 2005 - *Halite caves of the Atacama*. The NSS news. National Speleological Society, **63 (11)**: 4-19.

Frumkin A., 1992 - *The karst system of the Mount Seedom diapir*. Unpub. Ph.D. Diss. Hebrew Univ., 210 p. (in Hebrew)

Frumkin A., 1994 - *Hydrology and denudation rates of halite karst*. Journal of Hydrology, **162**: 171-189.

Frumkin A. & Forti P., 1997 - *Liquid Crystal Cave, Israel*. In: Hill C. & Forti P. (Eds.), *Cave minerals of the world*. Huntsville, National Speleological Society: 319-322.

Geršl M., Filippi M. & Bruthans J., 2008 - *Nález raftových stalagmitů v solném krasu v Íránu*.- 3th Conf. Kras, ČSS, Pratur, In: Speleoforum, **27**: 119-122 (in Czech with English summary).

Giurgiu I., 2005 - *Muntele recordului mondial*. Invitatie în Carpati, **51**: 3-18.

Gornitz V.M. & Schreiber B.Ch., 1987 - *Displacive halite hoppers from the Dead Sea: some implications for ancient evaporite deposits*. Journal of Sedimentary Research, **51 (3)**: 787-794.

Greenspan L., 1977 - *Humidity fixed points of binary saturated aqueous solutions*. J. Res. Nat. Bureau Standarts - A. Physics and Chemistry, **81 (1)**: 89–96.

Hill C.A. & Forti P., 1997. *Cave Minerals of the World*. Huntsville, National Speleological Society, 463 p.

Jeannel R. & Racovitza E.G., 1929. *Enumération des grottes visitées*. Arch. Zool. Exper. Gener. **68 (2)**: 293-608.

Lowry D.C., 1967 - *Halite speleothems from the Nullarbor Plain, Western Australia*. Helictite, **6 (1)**: 14-20.

Maltsev V.A., 1997 - *Stalactites, crystlactites, corlactites, tufl actites – 4 types of "stalactite-like" formations, generated from crystallization environments with different physical properties*. Proceedings of the 12th International Congress of Speleology, La Chaux-de-Fonds, Switzerland, 1: 267-270.

Maltsev V.A., 1998 - *Stalactites with "internal" and "external" feeding*. Proceedings of the University of Bristol Spelaeological Society, **21 (2)**: 149-158.

Naiman E.R., Bein A. & Folk R.L., 1983 - *Complex polyhedral crystals of limpid dolomite associated with halite, Permian Upper Clear Fork and Glorieta Formations, Texas*. Journal of Sedimentary Research, **53 (2)**: 549-555.

Palmer A.N., 2007 - *Cave Geology*. Allen Press, Lawrence, Kansas, U.S.A., 454 p.

Parkhurst D.L. & Appelo C.A.J., 1999 - *User's guide to PHREEQC (Version 2) – A computer program for speciation, batch-reaction, one-dimensional transport, and inverse geochemical calculations:* U.S. Geol. Surv. Water Resour. Investig. Rep. 99-4259, 143 p.

Pope M.C. & Grotzinger J.P. 2003 - *Paleoproterozoic stark formation, Athapuscow Basin, northwest Canada: rekord of cratonic-scale salinity cisis*. Journal of Sedimentary Research, **73 (2)**: 280-295.

Rimbach D., 1963 - *Salt coatings and salt beds in caves at Pisgah Crater, California*: Western Speleological Society, **26**: 1.

Rogers B.W., 1988 - *Noncarbonate minerals in Californi caves*. Proceedings of the National Speleological Society Convention, Hot Springs (South Dakota), 1-4.

Stepanov V.I., 1997 - *Notes on mineral growth from the archive of V. I. Stepanov (1924-1988)*. Proceedings of the University of Bristol Spelaeological Society, **21 (1)**: 25-42.

Struyf E., Smis A., Van Damme S., Meire P. & Conley D.J., 2009 - *The global biogeochemical silicon cycle*. Silicon, **1**: 207-213.

Talbot J.C., Stanley W., Soub R., & Al-Saudon N., 1996 - *Epitaxial reefs and mushrooms in the southern Dead Sea*. Sedimentology, **43**: 1025-1047.

Warren J.K., 2006 - *Evaporites: Sediments, Resources and Hydrocarbons*. Springer Berlin Heidelberg New York, Germany, 1035 p.

Watson A., 1985 - *Structure, chemistry and origins of gypsum crusts in southern Tunisia and central Namib Desert*. Sedimentology, **32**: 855-875.